BEARING FAULT MONITORING SYSTEM USING ACOUSTIC EMISSION

NUR ANIS NOR AZLAN

ELECTRICAL & ELECTRONICS ENGINEERING
UNIVERSITI TEKNOLOGI PETRONAS

JUNE 2010

Bearing Fault Monitoring System using Acoustic Emission

by

Nur Anis Binti Nor Azlan

FINAL DESSERTATION

submitted in partial fulfilment of

the requirements for the

Bachelor of Engineering (Hons)

(Electrical & Electronic Engineering)

JUNE 2010

Universiti Teknologi PETRONAS

Bandar Seri Iskandar

31750 Tronoh

Perak Darul Ridzuan

CERTIFICATION OF APPROVAL

Bearing Fault Monitoring System

using Acoustic Emission

By

Nur Anis Binti Nor Azlan

Final Dissertation

submitted to the

Electrical & Electronic Engineering Programme

Universiti Teknologi PETRONAS

in partial fulfilment of the requirement for the

BACHELOR OF ENGINEERING (Hons)

(ELECTRICAL & ELECTRONIC ENGINEERING)

Approved by,

____

(Dr. Rosdiazli bin Ibrahim)

Project Supervisor

UNIVERSITI TEKNOLOGI PETRONAS

TRONOH, PERAK

JUNE 2010

CERTIFICATION OF ORIGINALITY

This is to certify that I am responsible for the work submitted in this project, that the original work is my own except as specified in the references and acknowledgements, and that the original work contained herein have not been undertaken or done by unspecified sources or persons.

NUR ANIS BINTI NOR AZLAN

ABSTRACT

Electric motors are used in most modern machines. The observable uses would be in rotating machines such as fans, turbines and generators. Accidents involving mechanism and motor occurred in every part of the industry that utilizes machinery in the routine. Bearing fault is the common defects arise in many of cases. This project portrays a study of bearing fault monitoring system using acoustic emission. The objective of this project is to develop a bearing fault detection and diagnosis system to determine the condition of motor. The aim is to predict the cause of unhealthy bearing, hence improving the life span of the motor. The focus of this study is to monitor the condition of bearing's fault using acoustic emission sensor. The project commence with literature review where the focus is the damage of bearing and also the data acquisition and analysis of the system. The acoustic emission sensor will be mounted on the motor. The noise emitted from the source will be captured by acoustic emission sensor. The signal retrieved from the sensor will be connected to USB 1208 FS (Data Acquisition Card) which is link to a computer. Eventually, the signal is being analyzed to predict whether the signal is healthy or unhealthy. Various analyses from different type of motor are done by MATLAB software and placed in a database for monitoring and references purposes.

ACKNOWLEDGEMENT

First and foremost, praise to Allah S.W.T. for His blessings and because of Him, this project managed to be completed and finished on time. Her deepest appreciation to the supervisor of the project, Dr. Rosdiazli bin Ibrahim for his assistance and support throughout the execution of the project.

The author would also like to thanks the Final Year Project committee for giving a great opportunity for us to operate our own project. Final year project is also a platform to learn new things. The author would like to express her gratitude to all lecturers, UTP staff and post graduate students that have contributed directly or indirectly in accomplishment of the project. Last but not least, my family and fellow friends for continuous support and motivation for these two semesters.

TABLE OF CONTENTS

LIST OF FIGURES

LIST OF TABLE

LIST OF ABBREVIATIONS

AE	Acoustic Emission
HP	Horse Power
SPM	Shock Pulse Method
DAQ	Data Acquisition System
RPM	Revolution per minute
FFT	Fast Fourier Transform
UTP	Universiti Teknologi Petronas
RMS	Root Mean Square

CHAPTER 1

INTRODUCTION

1.1 Background of Study

Electric motor problems take place for a variety of reasons, ranging from basic design faults and insufficient manufacturing quality to problems trigger by application and the location conditions which lead to motor failures. Majority of motor failures caused by combination of defection of motor parts namely bearing, winding, shaft etc. If these problems are kept within the design capabilities of the system, failure would not take place. Nevertheless, if any combination of them exceeds the design capacity, then the condition of the motor may become severely shrink and a catastrophic failure could strike. Therefore, detection of any deviation and fault in electric motor at the beginning stages is crucial for industrial plant and equipment to prevent unplanned shutdown which is very costly. Through condition monitoring, the defect of the motor can be detected and the source of fault can be identify.

Motor fault analysis is the study of several of defection that can occur in electrical motor to ensure that the developed fault of the equipment are less than the allowable capabilities under operating conditions of a particular system and even during the worst operating conditions. Detection and analysis of bearing fault is the focus of the study. Acoustic emission (AE) techniques would be used as a detector to monitor the motor condition. The AE monitoring system can capture elastic wave signals produce at the site defection of the motor. The attain signals would be processed and analyzed to expose the information of the processed that is being monitored.

1.2 Problem Statement

Atypical noise portrays something amiss in particular equipment. These noise created corresponds to defect of parts of the motor that can lead to motor failure. Maintenance implementation and proper schedule for maintenance is crucial for early detection of fault. Early detection of some parts of the motor allows replacement for the certain tool rather replacement of the motor. For example, a 100 hp, three-phase ac motor costs approximately US$7500. The replacement ball bearings for the same motor cost approximately US$250 [1]. This indicates that the corrective maintenance is high and it may lead to disturbance or shut down of the plant if the discovery of the faulty is too late. In addition, there is no proper troubleshooting tool available that can detect the fault in initial stage. To overcome these problems, one needs to determine on which tool that creates the unwanted sound. In reply to this, the project would be focusing on bearing as this defect is the most common defect in motor that contribute to motor failure.

1.2.1 Problem Identification

This project requires the identification of the motor defects. The focus of the motor defects would be bearing fault. Acoustic emission technique is the technique used for condition monitoring. The noise from the defect's part of the bearing would be capture using acoustic emission sensor. The pattern of AE signals will be store and analyzed using MATLAB. The system should be able to provide early detection prior to the fault generated. Additionally, it should also be able to identify the type of fault in the bearing.

1.3 Objectives

The objective of the project is to develop fault detection and diagnosis tools that can be used:

1. To detect the defection of the bearing fault using acoustic emission technique.
2. To predict the possible cause of unhealthy bearing.
3. To develop a set of database based on condition of the bearing.

1.4 Scope of Study

The scope of the study is to capture the noise produced by the bearing using acoustic emission sensor. The noise emitted from the source will be capture by acoustic emission sensor and convert it to utilizable electrical signal. The equipment will be setup for testing actual motor condition. With the objectives stated, the project is feasible and manages to complete in 2 semester duration.

CHAPTER 2

LITERATURE REVIEW

2.1 Theory

This section describes the type of motor fault that is commonly arising in many of cases. A surveys show that bearing failures are the main cause of all failures which is 50% and stator winding failures about 15 to 35%, depending on the application. The overall percentage of rotor defect and shaft failures is below 10% [33].

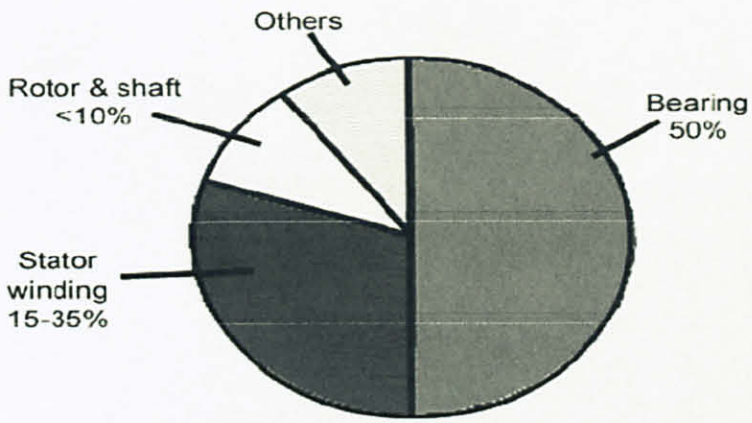

Figure 2.1: Motor faults.

2.1.1 *Bearing Fault*

Rolling element bearing condition monitoring has received considerable attention for many years because majority of rotating machines are caused by faulty bearing [2]. Rolling element bearings divided into inner raceways, outer raceways and rolling elements rotating between inner and outer raceways [30]. Under normal operating condition, fatigue failure begins with a small fracture which is located below the surface of raceways and rolling elements. The fracture begins to spread to the surface producing detectable vibration and increasing noise levels [3]. Such damage, known as primary damage, gives rise to secondary, failure-inducing damage such as flaking and cracks [14]. Once started, the affected area expands rapidly contaminating the lubrication and causing localized overloading over the entire circumference of the raceway [3]. This is the common mode that causes the bearing to fail. There are many other conditions that results the bearing to fail such as improper lubrication, improper installation, dirt ingression etc.

There are five basic frequencies that are used to describe the dynamic of elements bearing which is shaft rotation frequency (F_S), cage frequency (F_C), ball pass outer raceway frequency (F_{BPO}), ball pass inner raceway frequency (F_{BPI}) and ball spin frequency (F_B) [22]. A healthy bearing condition can have F_{BPO}, F_{BPI} and its harmonics but the amplitude of the signal is small and smooth. When inner raceway and outer raceway defects appear in the bearing, F_B, F_{BPI}, F_{BO} and their harmonics are exited correspondingly [30].

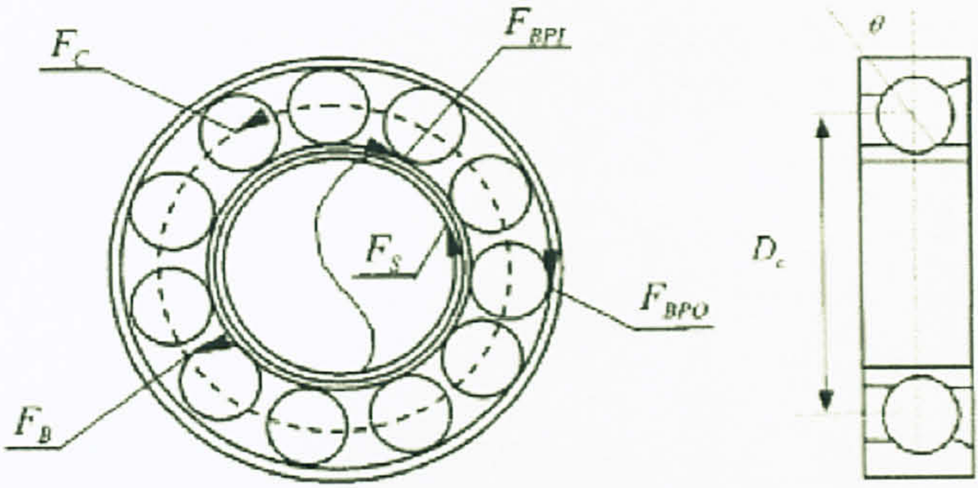

Figure 2.2: Cross section of bearing

The expressions of these frequencies are expressed as follows:

$$F_C = \frac{1}{2} F_S (1 - \frac{D_b Cos\,\theta}{D_c})$$

$$F_{BPO} = \frac{N_B}{2} F_S (1 - \frac{D_b \cos\theta}{D_C})$$

$$F_{BPI} = \frac{N_B}{2} F_S (1 + \frac{D_b \cos\theta}{D_C})$$

$$F_B = \frac{D_C}{2D_B} F_S (1 - (\frac{D_b \cos\theta}{D_C})^2)$$

where D_b is the ball diameter while D_c is the bearing pitch diameter and θ is the contact angle of the bearing [22].

Also, stator current monitoring can detect bearing defect in induction motors. Line current spectral components are predicted at frequencies of:

$$F_{bng} = |F_e \pm mF_V|$$

where Fv is one of the characteristic vibration frequencies while Fe is the supply frequency; m=1,2,3..etc. Even though the magnitudes of the harmonic components are small to other spectral component, however, they fall at diverse spot from those of the supply and natural machine slot harmonics. This occurrence makes it easy to differentiate between a healthy and defect operation [31].

Dirt ingression and corrosion are the two modes that speed up bearing failure due to severe condition being practiced in the industrial site [3]. Unknown particles that presents in the bearing contaminate the bearing lubrication. Small, abrasive particles, such as grit or swarf that have entered the bearing by some means or other, cause wear of raceways, rolling elements and cage [14].

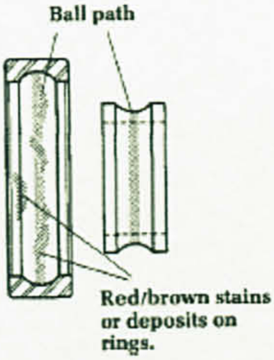

Figure 2.3: Corrosion on the bearing [29].

Improper lubrication also contributes to bearing failure. The purpose of the bearing lubrication is to prevent direct metallic contact between the various rolling and sliding elements [12]. Grease lubrication is the method most commonly used on small and medium size electric motors in the range of 1 to 500 HP for horizontal machines [13].

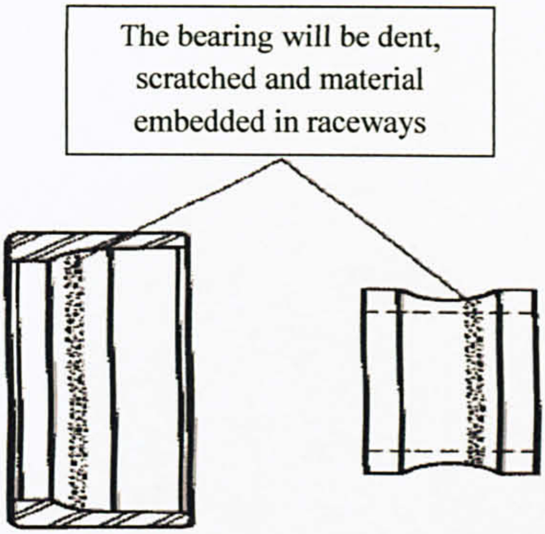

Figure 2.4: Failure in lubrication [29].

Figure 2.5: Insufficient lubrication [29].

Improper installation happened because incorrect way of applied force when connecting the bearing into the shaft or the housing. This produce high tension on the v belt drives t leads to higher bearing temperature and shorter lifetime of the bearing [12]. Besides that, the coupling half that is not balanced correctly and misalignment of the rolling element bearing also contributes to improper installation [3,12].

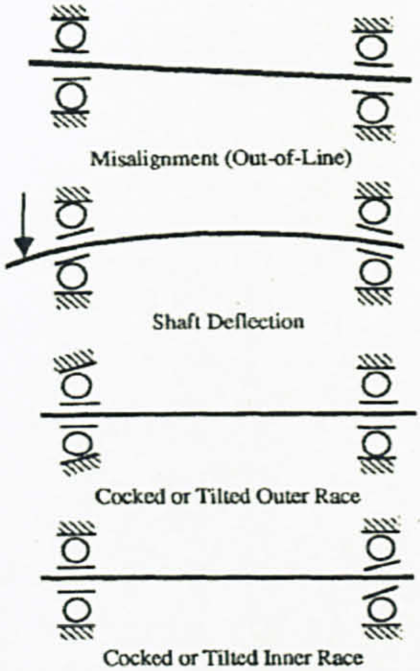

Figure 2.6: Types of rolling element bearing misalignment [3].

2.1.1.1 Categorization of bearing fault

Single-point defect is classified as a single, localized defect on a good bearing surface. The defect produces one of the four characteristic fault frequencies depending on which surface of the bearing contains the fault. Common example of the defect is a pit or spall. A bearing can also possess multiple single-point defects [21]. Single point defect produces certain characteristic of fault frequencies to develop and vibrate surrounding the machine. The frequencies of these components occur are predictable and it depends on the surface of the bearing that has the defect [22].

Generalized roughness is a defect where the surface of the bearing has decay and expanded which produce the surface of the bearing to be deformed, rough. There is no localized defect in which to recognize the location that initiates the fault. It is a large area of the bearing surface that has deteriorated [21]. Example of the generalized roughness fault is the overall surface roughness produced by a contamination or poor lubrication. The consequences caused by generalized roughness are difficult to predict, and there are no characteristics fault frequencies with this sort of fault [23].

2.1.2 Stator Winding Fault

There two criteria that cause the stator winding failure. First would be due to gradual deterioration of electrical insulation. High temperature of stator winding cause the insulation layer depreciates over time which leads to an increase in air pockets in the insulation that allows copper conductors to vibrate [32]. As a result, the insulation become worse and short circuit occurs in the winding due to the vibration of copper conductors [30]. Second is because of looseness of the windings in the slots. The gap between looseness may cause the winding coil to vibrate in slot. The vibration will scrape in insulation surface and lead to failure [32].

2.1.3 Rotor Faults

The cause of rotor faults is mainly because a massive breakage of joints between bars and end rings as a consequence of pulsating load or direct on line starting. Current increases in the remaining bar with a risk of fractures [18].

For a broken rotor bars, sideband vibrations are expected which can detected around fundamental rotor frequency. The expression of sideband frequency is as follow:

$$f_b = (1 + 2ks) f$$

Where k is 1, 2, 3…., s is the slip and f is the rotor frequency [30]. A motor with broken rotor bar will develop higher sideband amplitude around the fundamental frequency compare to a normal motor [32]. When the motor is healthy, there would be no sidebands visible [30].

2.1.4 *Shaft Defect*

Shaft signals of electric rotating machines offer potentials for defect detections [4]. The main reasons of shaft defects are overload, fatigue and corrosion. Shafts are experience cyclic load conditions, are difficult to access for maintenance and are vulnerable to cracks nucleation and growth [5]. Wherever there is a surface discontinuity, such as bearing shoulders, snap ring grooves, keyways, shaft threads, holes, shaft damage or corrosion a stress raiser will be present. The common area for shaft defect is on the part of the shaft from point *H–K*. Although in most cases where an axial load will result first is in a bearing failure, there are numerous examples where the shaft is damaged before the motor is stopped (Figure 5) [6].

Table 2.1: Common causes of shaft failure for motor [6].

Failure Mode	Cause
Overload	High impact or loading (quick stop or jam).
Fatigue	Excessive rotary bending, such as overhung load or high torsional load or damage causing stress raisers.
Corrosion	Wear pitting, fretting and/or cavitation can result in a fatigue failure if severe enough.

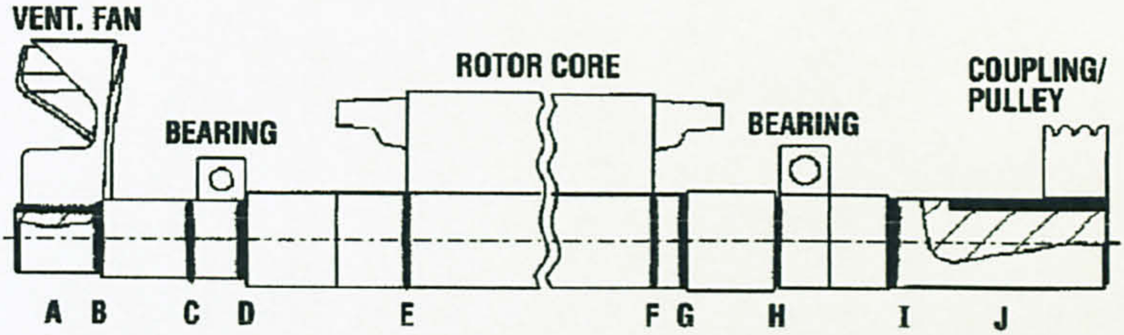

Figure 2.7: Typical rotor assembly cross section.

2.2 Condition Monitoring Technique

Condition monitoring technique is most commonly technique used to detect early defect in rotating machines. By condition monitoring, the sudden shut down of the plant during critical operation can be prevented. Many condition monitoring techniques has been implemented in the industry. The typical techniques used for condition monitoring rotating machines are vibration monitoring, acoustic emission, stator current and Shock Pulse Method (SPM). Based on literature review, acoustic emission is proved to be the best technique compared from the techniques mentioned [15].

2.2.1 Vibration monitoring

Machines deteriorate over times. Ultimately, machines will produce vibration and increasing in noise levels on the exact location of the faulty. Vibration monitoring is effective in detecting fault in machines, but only in specific part of the motor. More sensors required to detect faulty in one machine. While some large motors may already come with vibration transducers, it is not economically or physically feasible to provide the same for smaller machines [6]. This means that small to medium size motors must be checked periodically by portable equipment that moves from machine to machine [6]. Normally, the machine faults and problems can be detected and identified by comparing the signals for the machine running in normal and abnormal condition [7].

2.2.2 Acoustic emission

Generally most materials emit some level of seismic signals when subjected to stress or deformation [7]. Acoustic emission (AE) is the phenomenon of transient elastic wave generation in materials under stress [9]. These elastic waves generated due to mechanisms such as crack, deformation, damage, friction and etc [11].AE technique is, therefore, widely used in nondestructive testing for the detection of crack propagation and failure detection in rotating machinery [9]. The signal is generated and measured in the frequency range which is greater than 100 kHz [9]. Example of operation, during the bearing operation, bursts of acoustic emissions (AE) result from the passage of the defect through the roller and raceway contacts [10]. Damages at variety locations of a bearing (inner race, roller and outer race) will have characteristic frequencies at which bursts are generated. Thus, the signal of a damaged bearing consists of periodic bursts of AE. The signal is usually considered to be amplitude modulated at the characteristic defect frequency [10].

2.2.3 Shock Pulse Method (SPM)

Bearing surfaces always have a degree of roughness. When the bearing rotates, this surface roughness or a surface defect will cause mechanical impacts. These mechanical impacts produce shock pulses causing the bearing to act as a "shock pulse generator" [20]. The shock pulses caused by the impacts in the bearings initiate damped oscillations in the transducer at its resonant frequency. Shock Pulse Monitoring (SPM) applies piezo-electric transducers fixed to the bearings to detect shock waves caused by impact between moving parts and defect parts, a crack on the inner and outer race or on the rolling elements in the bearing [18]. Measurement of the maximum value of the damped transient gives an indication of the condition of rolling bearings [17]. The maximum normalised shock value is a measure of the bearing condition [15]. However, some investigators have reported that the method could not effectively detect defects at low speeds [17]. The maximum normalised value of SPM is almost three times less effective as compared to AE technique [15].

2.2.4 Stator Current Technique

The relationship of the bearing vibration to the stator current spectra can be determined by remembering that any air gap eccentricity produces anomalies in the air gap flux density [15]. In the case of a dynamic eccentricity that varies with rotor position, the oscillation in the air gap length causes variations in the air gap flux density [3]. Since ball bearings support the rotor, any bearing defect will produce a radial motion between the rotor and stator of the machine [15]. Current monitoring is non-invasive, and may even be implemented in the motor control center remotely from the motor being monitored. The major disadvantage of current- monitoring is that bearing-fault signatures are subtle in the stator current where the dominant components are supply frequency components [19]. However, stator current monitoring has the advantage that it requires minimum instruments and is sometimes referred to as sensor-less technique [15].

2.2.5 Comparison between AE technique and vibration monitoring

Vibration measurement can locate the location of the defect but the direct vibration spectrum may not be able to detect the defection in the initial stage [17]. The frequency spectrum of vibration readings failed in the majority of cases to identify the defect frequency or source [16].

AE technique is widely used in nondestructive testing for the detection of crack propagation and failure detection in rotating machinery. AE parameters can detect defects before they appear in the vibration acceleration range and can also detect the possible sources of AE generation during a fatigue life test of thrust loaded ball bearings [9].

AE was more sensitive than vibration to variation in defect size, and no further analysis of the AE response was required in relating the defect source to the AE response, which was not the case for vibration signatures [16].

AE transient bursts could be related to the defect and that AE levels increase with increasing speed and load [16]. In general the difference in AE maximum peak amplitude of healthy and smallest defect size is quite significant and makes it possible to detect the presence of a defect for diagnosis easier at the early stage in comparison with other condition monitoring techniques [15].

2.3 Analysis

2.3.1 Amplitude Response

Amplitude response is the maximum output amplitude obtained over various points in the frequency range of an instrument operating under rated conditions. Good bearings at low event emission occurs over a narrow range of peak while, the defect bearing, it is observed that there is a rise in event emission and the emission takes place in a wider range [9].

The amplitude of an AE signal from the work station is decrease significantly during AE acquisition from work station to tool probably due to reflection of interface. The friction between workstation and tool and the tool fracture can be observed as the most important sources of continuous and transient AE signals during turning. Thus, the amplitude of the continuous-type AE signal could be used to monitor the incipient stage of defection [24].

2.3.2 Statistical Analysis

Peak level, kurtosis analysis, and root mean square (RMS) value are the examples of statistical analysis [2]. Kurtosis is a parameter that calculates 4^{th} moment of probability density functions. The probability density function is given by:

$$M_x = \int_{-\infty}^{+\infty} x^n P(x)\, dx \quad n = 1, 2, 3, \ldots, m,$$

Kurtosis is a measure of the impulsive nature of the signal [34]. . It is a global signal statistic which is highly sensitive to the spikiness of the data [35]. Kurtosis is an important parameter that is used in engineering for detection of symptoms of defection due to its sensitivity to high amplitude events. Kurtosis techniques are widely used in crack detection in isotropic plates and also modulation classification of communication signals [27,28].

Kurtosis expression is given by:

$$\beta_2 = \frac{\int_{-\infty}^{+\infty} (x-\bar{x})^4 P(x)\, dx}{\sigma^4},$$

Kurtosis value that does not exceed 3.0 proved that the bearing is in a good condition, while for kurtosis that exceed 3.0, it indicates that the tool is in failure [7,17]. The kurtosis value increases with bearing defect severity [16]. However, there are cases that kurtosis value goes down as the damages increases over time. Thus, the status of RMS value will be compute to validate the condition of deteriorate tool. Root mean square (RMS) will increase with the increase of defection [25].

CHAPTER 3

METHODOLODGY AND PROJECT WORK

3.1 Procedure Identification

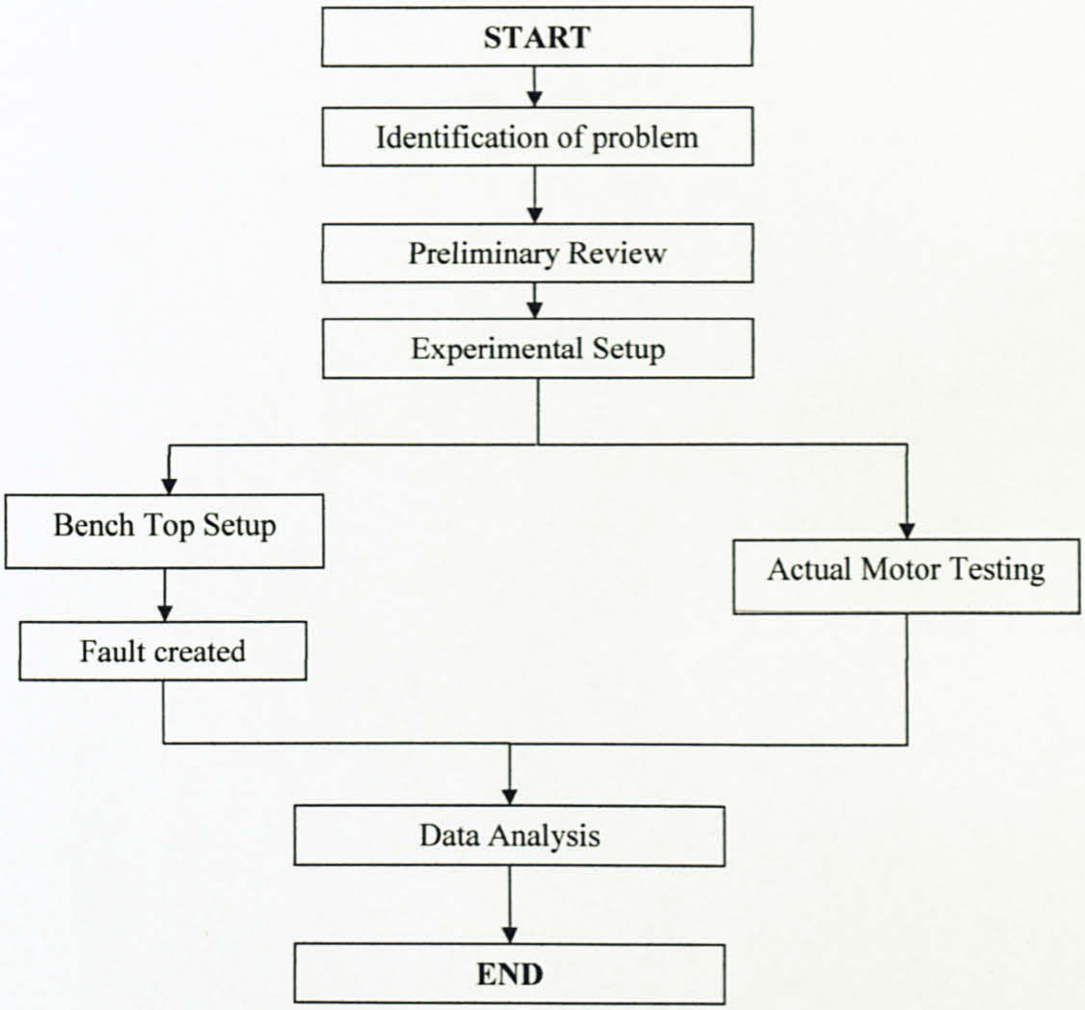

Figure 3.1: Flowchart of the project.

3.1.1 Preliminary Review

Preliminary research consists of literature review and tools that will be used for this project. Literature review comprises of journals, books and technical magazine. Research for the tools of the project requires information from practical books as well as journals for selection of the proper tools that is feasible for this project.

3.1.2 Experimental Setup

Experiment setup is divided into two parts which are bench top setup and actual motor testing.

3.1.2.1 Bench Top Setup

In bench top setup, the fault of the bearing will be created. The signal acquired from the setup will be stored and analyzed. The objective of the setup is to gather as many signals from several of bearing fault created to generate a library of signals of bearing faults.

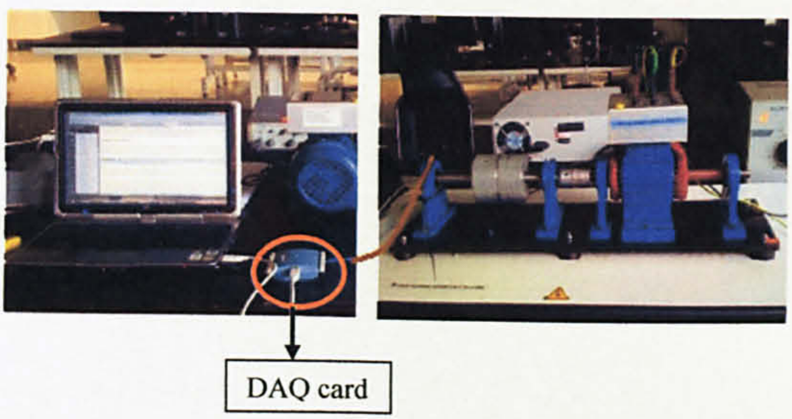

Figure 3.2: Experimental Setup

3.1.2.2 Actual Motor Testing

For actual motor testing, the sensor will be attached to the bearing housing of the motor. The signal retrieved from the electrical motor will be stored and analyzed. The objective of the testing is to compare the signal from the motor with the signal from the bench top setup to predict the type of fault take place in the electrical motor.

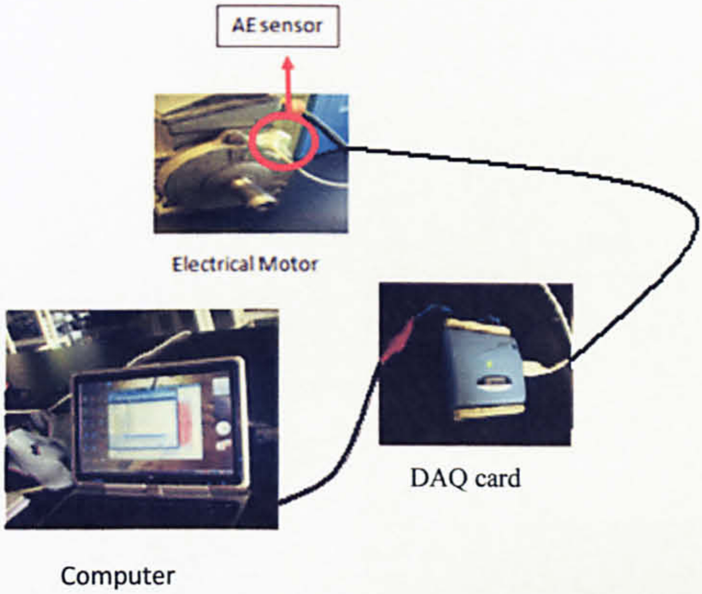

Figure 3.3: Actual motor testing

3.1.3 Data Analysis

The data acquired from the sensor will be retrieved using DAQ card (Data Acquisition System). When the data acquisition completed, the signals received will be process using MATLAB software. The signals will be converted to electrical signal for analysis and reference.

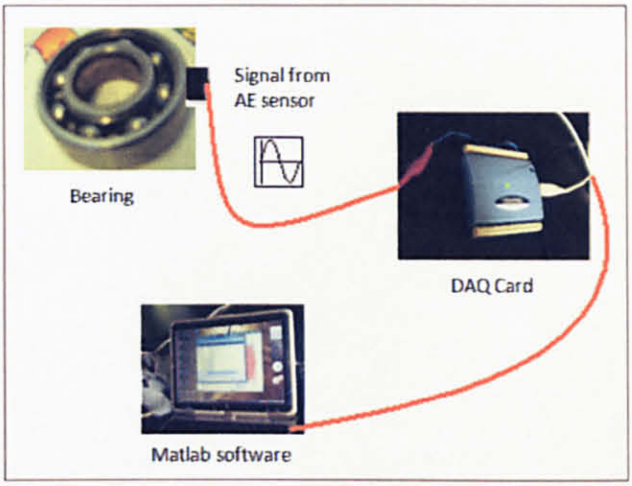

Figure 3.4: Schematic of project setup.

3.2 Tools and Equipments

Tools identification is divided into hardware and software that are required for this project.

3.2.1 Hardware

Hardware used for the experimental setup is as below:

- Acoustic Emission Sensor
  - Specification as in APPENDIX VI.
- Data Acquisition Card (DAQ)
  - Specification as in APPENDIX VI.
- Computer

3.2.2 Software

Software used for the experimental setup is as below:

- MATLAB
  - Simulink

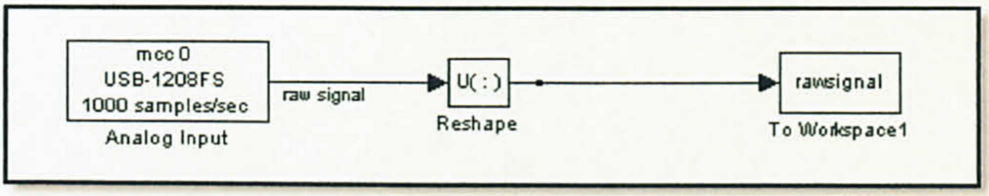

A simple simulation is constructed using Simulink, MATLAB for data acquisition from the DAQ card.

CHAPTER 4

RESULTS AND DISCUSSION

4.1 Results

The most representative of ball bearings is deep groove ball bearing. There are three types of deep groove ball bearing that are used and tested for the project which are open (c), Z (b) and RS (a). Experiments were conducted based on type of bearing used with 5kg load.

a b c

Figure 4.1: Ball bearing type 6203RS (a), 6203Z (b), and open (c).

4.2 Results: Bench Top Setup

4.2.1. Experiment 1: Ball bearing model 6203 Open

There are two conditions created for the particular bearing which is healthy and poor lubrication. The two bearings were tested on bench top setup at 60V, at speed 1190 rpm for 5 minutes. Below are the time domain data and magnitude response generated for the experiment.

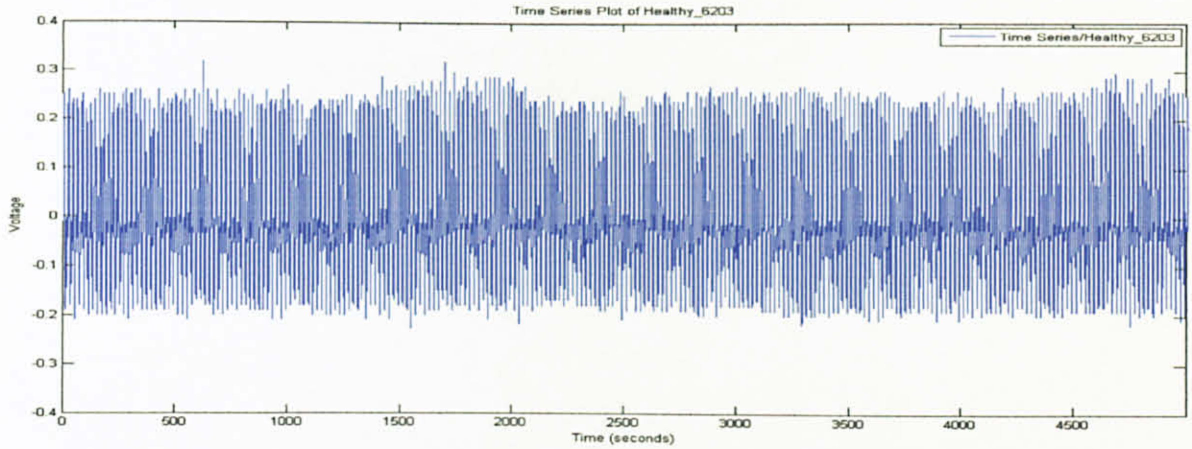

Figure 4.2: Time domain data from good ball bearing (6203 Open).

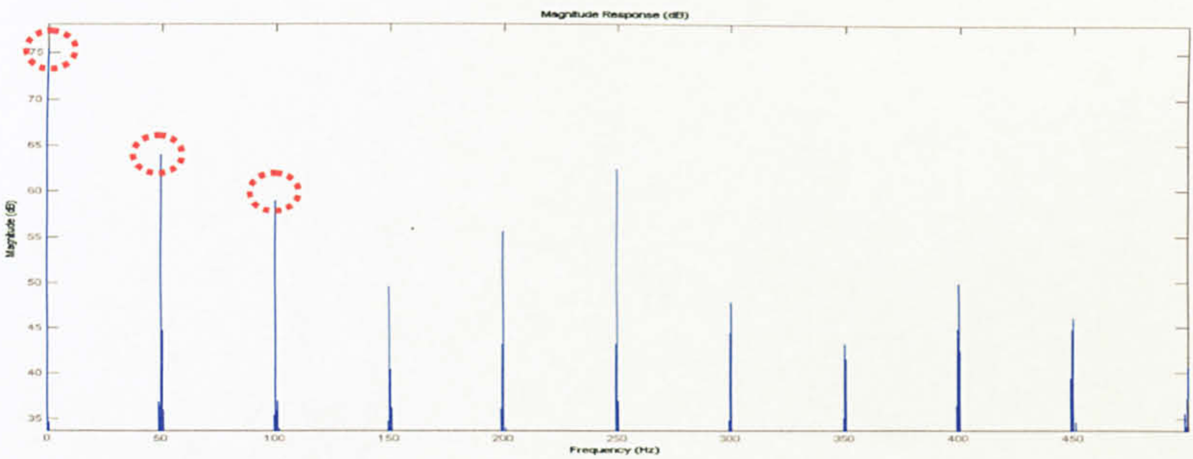

Figure 4.3: Magnitude response from good ball bearing (6203 Open).

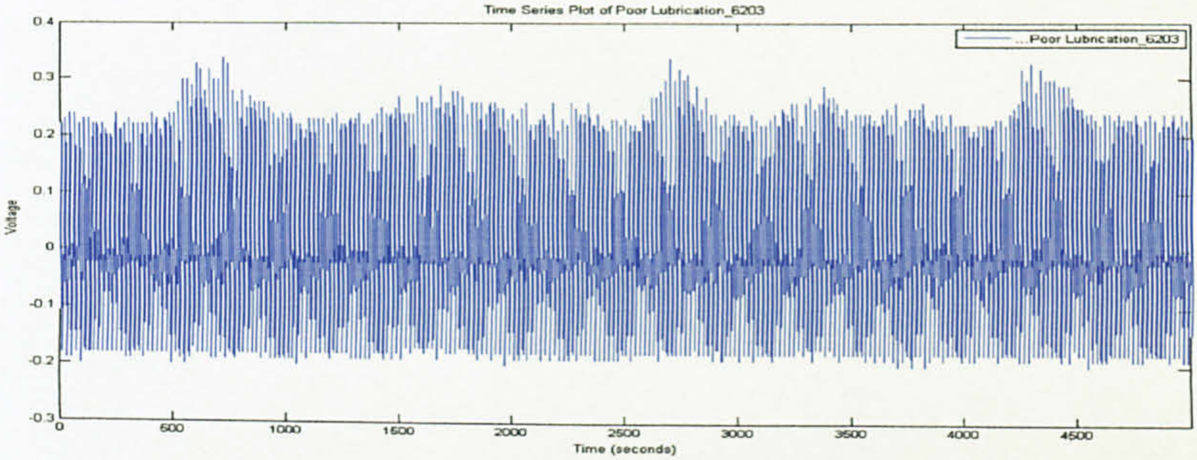

Figure 4.4: Time domain data from poor lubricate ball bearing (6203 Open)

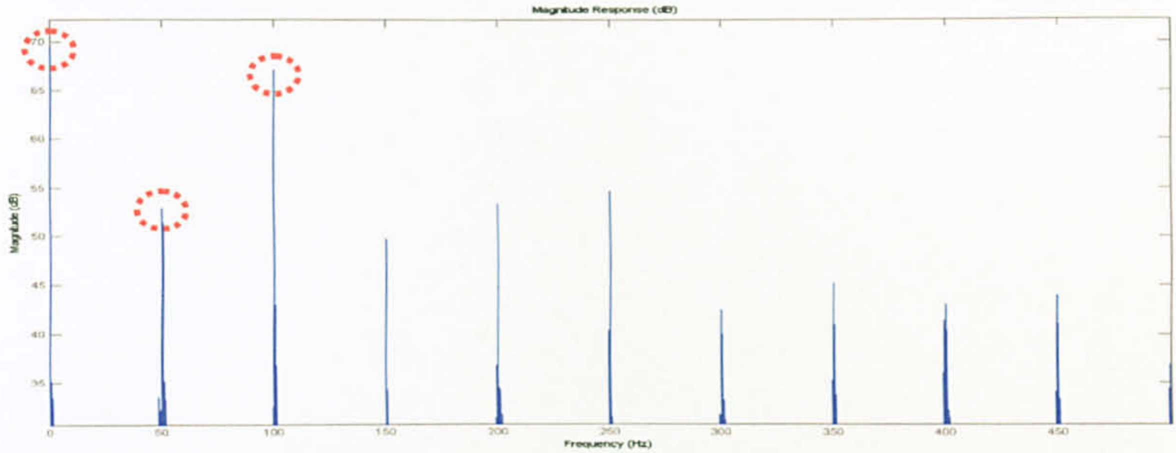

Figure 4.5: Magnitude response from poor lubricate ball bearing (6203 Open)

4.2.2. *Experiment 2: Ball bearing model 6203Z*

There are three conditions created for the particular bearing which is healthy, poor lubrication and inner defect. The two bearings were tested on bench top setup at 60V, at speed 1190 rpm for 5 minutes. Below are the time domain data and magnitude response generated for the experiment.

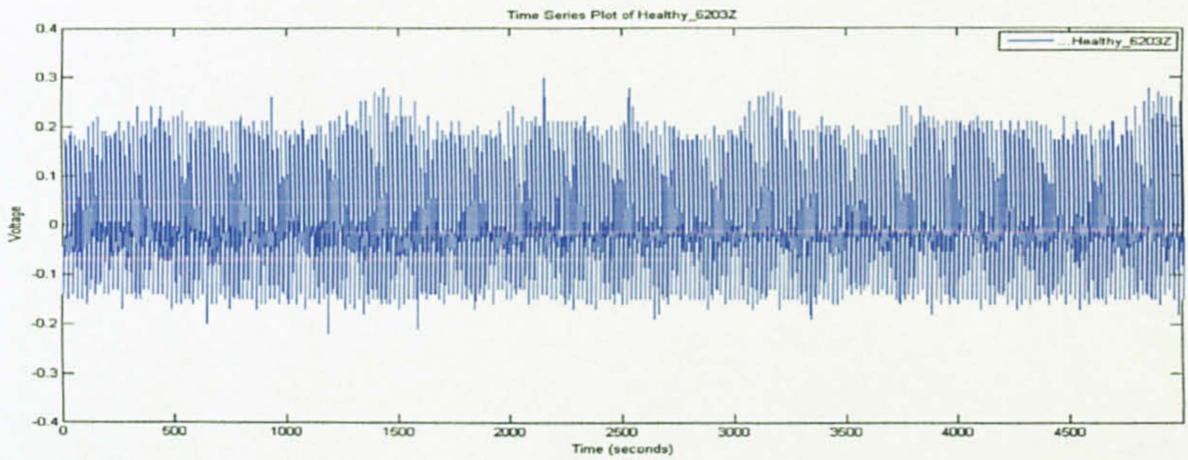

Figure 4.6: Time domain data from good ball bearing (6203Z)

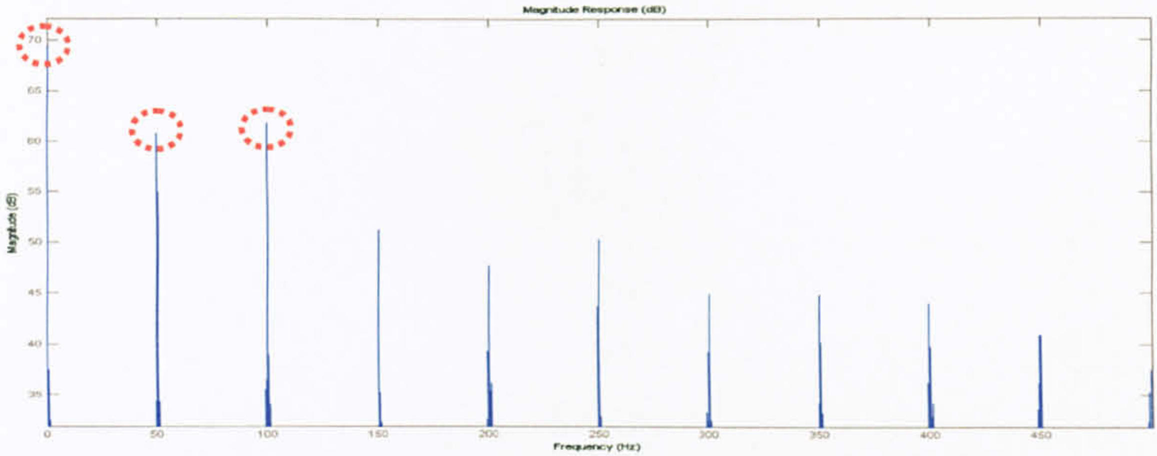

Figure 4.7: Magnitude response from good ball bearing (6203Z)

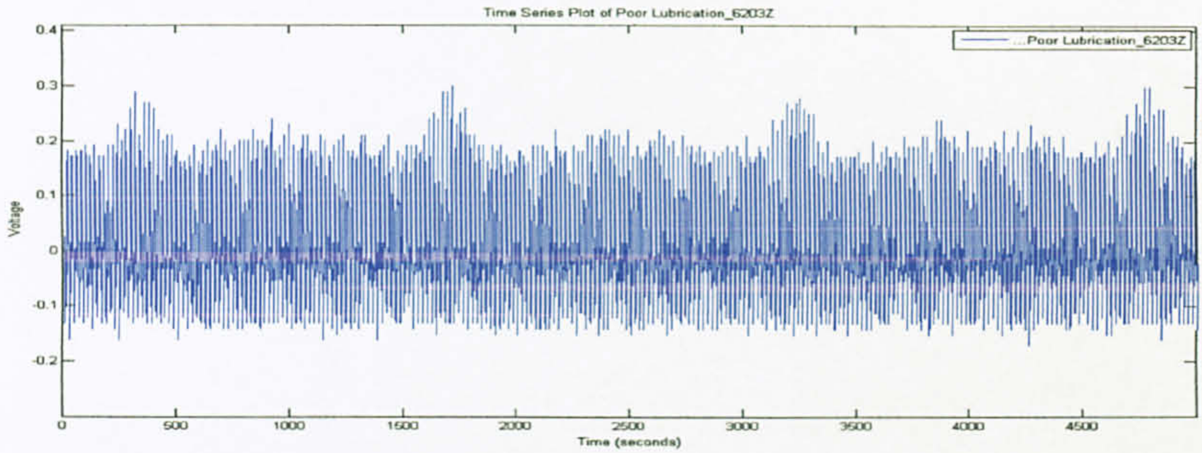

Figure 4.8: Time domain data from poor lubricate ball bearing (6203Z)

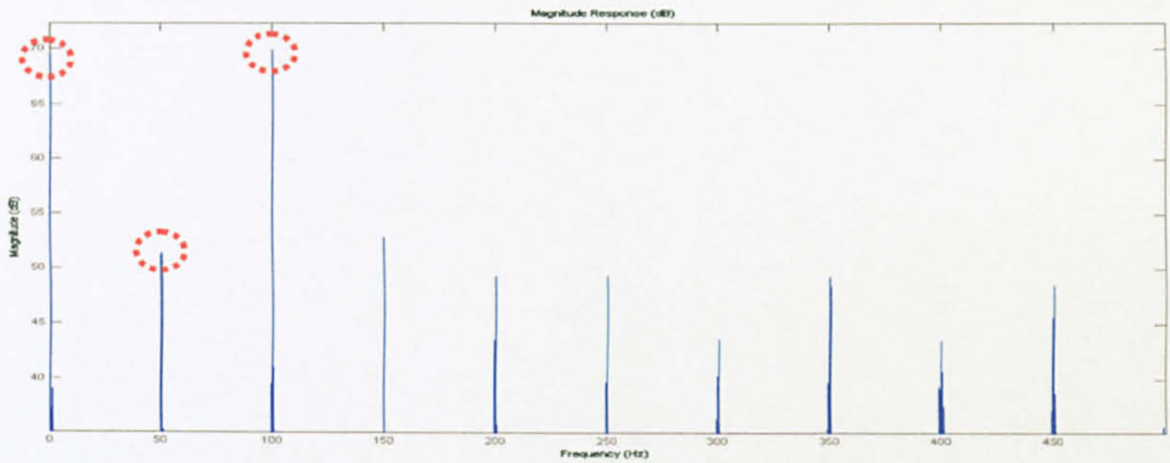

Figure 4.9: Magnitude response from poor lubricate ball bearing (6203Z)

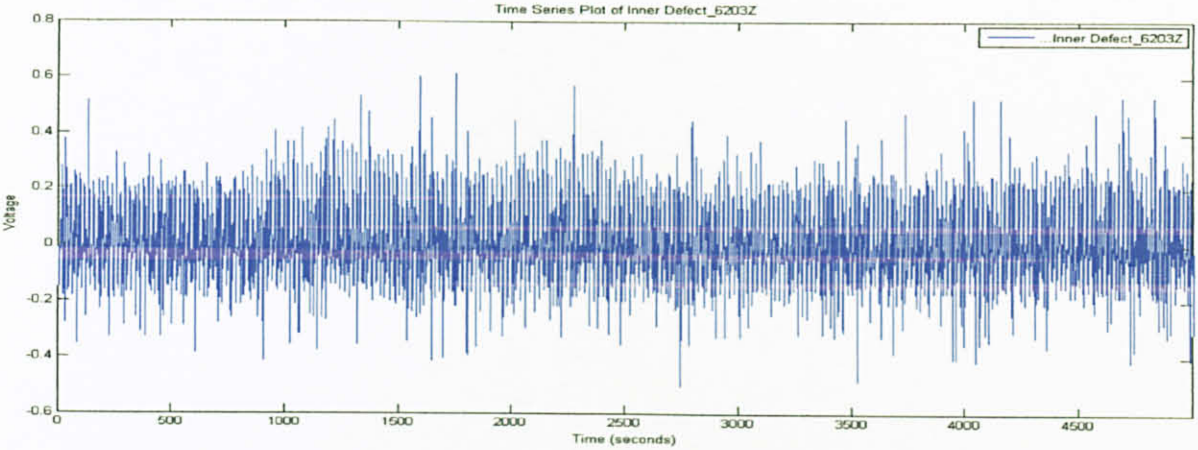

Figure 4.10: Time domain data from inner defect ball bearing (6203Z)

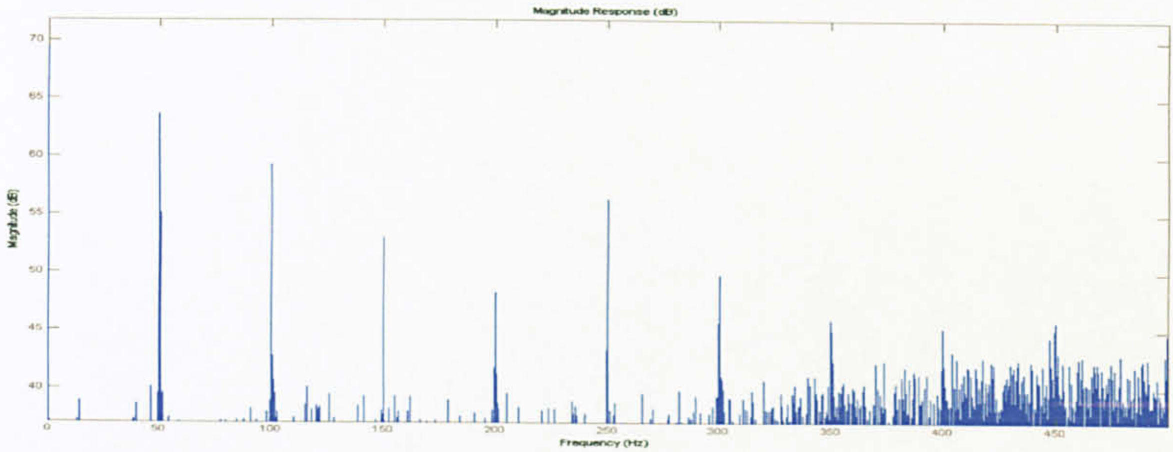

Figure 4.11: Magnitude response from inner defect ball bearing (6203Z)

4.2.3. *Experiment 3: Ball bearing model 6203RS*

The bearing was tested in healthy condition. The bearing was tested on bench top setup at 60V, at speed 1190 rpm for 5 minutes. Below are the time domain data and magnitude response generated for the experiment.

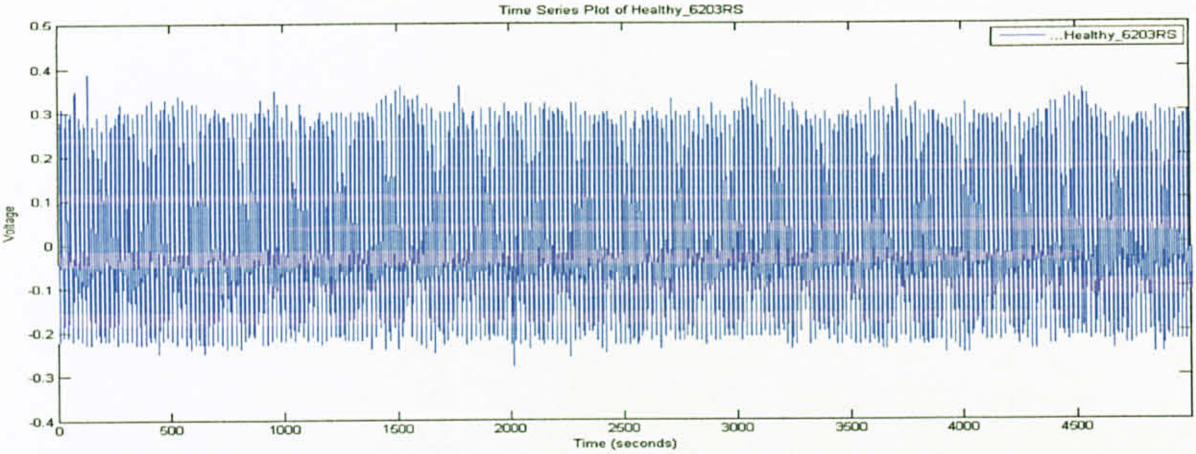

Figure 4.12: Time domain data from good ball bearing (6203RS)

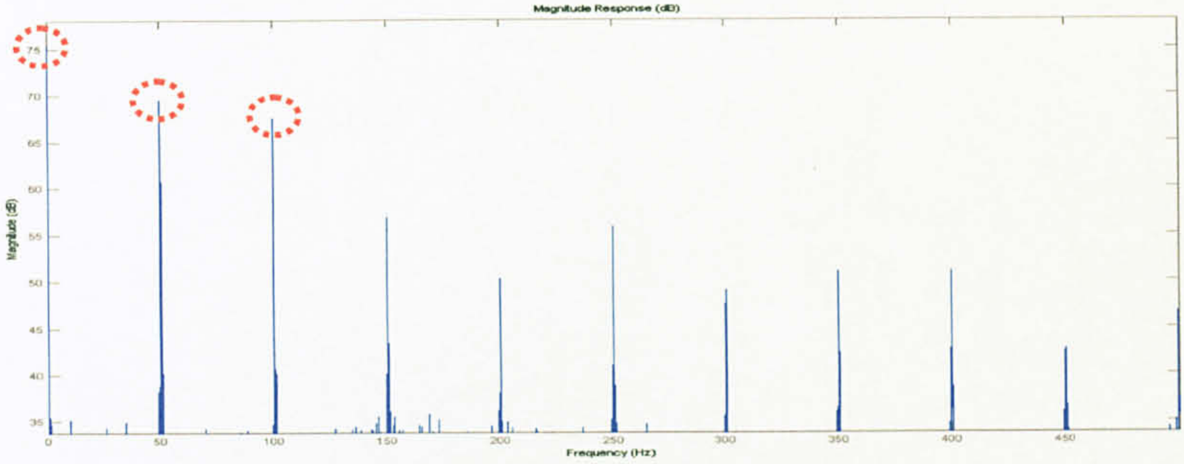

Figure 4.13: Magnitude response from good ball bearing (6203RS)

4.3 Discussion: Bench Top Setup

The results for bench top setup are represented in three forms which are time domain, magnitude response and statistical analysis. It is taken based on three types of bearings accordingly. Below are the analyses of the results which are divided into three categories:

a) Healthy
b) Poor lubrication
c) Inner defect

4.3.1. Bearing Condition: Healthy

Table below indicates the summary of signals for healthy bearings.

Table 4.1: Healthy bearings.

Time Domain	Magnitude Response
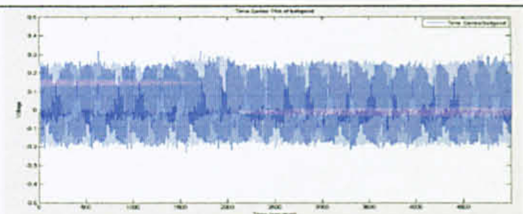	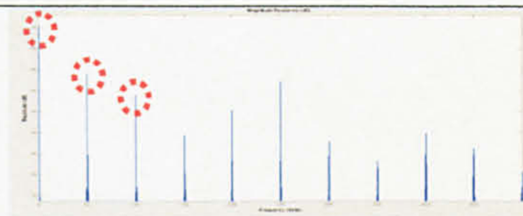
Type of bearing: 6203 Open	
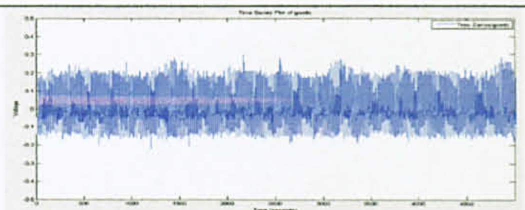	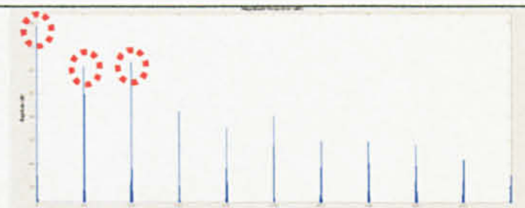
Type of bearing: 6203Z	
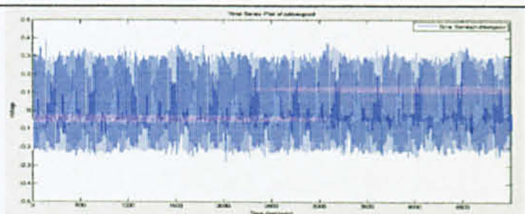	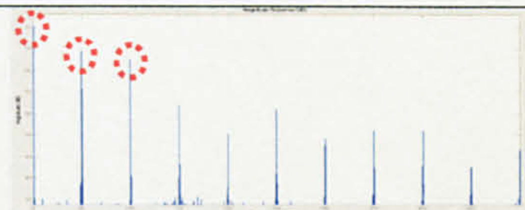
Type of bearing: 6203RS	

Based on the table above, indicate the time domain and amplitude response for healthy bearings. The signal in time domain is stable with minimal peak. In magnitude response, a similar significant pattern has developed from three different types of healthy bearings. The signature of magnitude response can be observed by the first three peaks in the magnitude response from three different bearings.

4.3.2. Bearing condition: Poor lubrication

Table below indicates the summary of signals for poor lubrication bearings.

Table 4.2: Poor lubrication bearings.

Time Domain	Magnitude Response
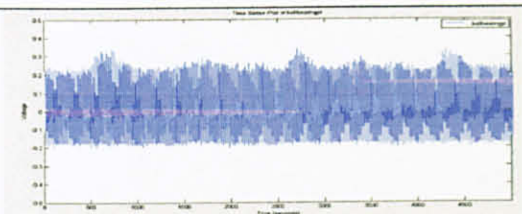	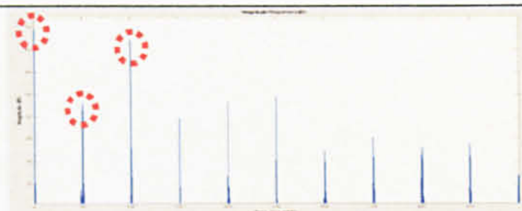
Type of bearing: 6203 Open	
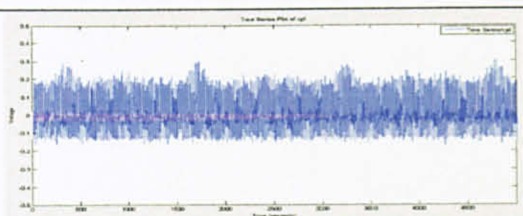	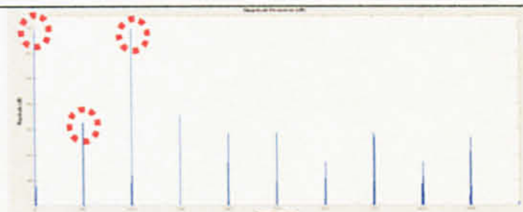
Type of bearing: 6203Z	

The table above, indicate the time domain and amplitude response for poor lubrication bearings. The signals in time domain for unhealthy bearings have a few peaks after certain durations compare to the healthy signals. In magnitude response, there is a similar signature generated from poor lubrication defect from two different types of bearings. The first three peaks were observed. The level of second amplitude is a quite short compared to the first and third peak.

4.3.3. *Bearing condition: Inner defect*

Table below indicates the summary of signals for inner defect bearings.

Table 4.3: Inner defect bearings.

Time Domain	Magnitude Response
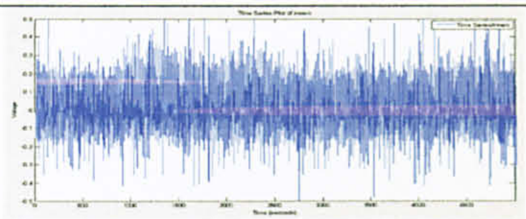	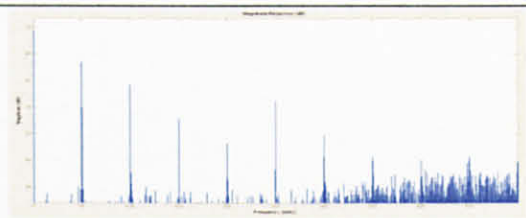
Type of bearing: 6203Z	

The condition of bearing is unhealthy and it cause by inner defect of the bearing. The inner defect collides with the roller ball inside the bearing which resulted more noise. It is showed in the pattern from the time domain signal. Also, the noise can be seen in few last peaks of the magnitude response.

4.3.4. *Statistical Analysis*

Below is the statistical analysis for three different condition of bearing.

Table 4.4: Statistical analysis for bearings.

Type of Bearing	**Bearing Condition**	**Kurtosis**	**RMS**
6203Open	Healthy	2.15	0.0297
6203Open	Poor Lubrication	2.225	0.0407
6203Z	Healthy	2.3477	0.0329
6203Z	Poor Lubrication	2.469	0.0411
6203Z	Inner	3.9977	0.0453
6203RS	Healthy	2.128	0.0336

The above table shows the kurtosis and RMS value for three different bearings according to the condition. The value of kurtosis increase as the bearing began deteriorating. The kurtosis value for poor lubrication condition for both bearing (6203 Open and 6203Z) are below 3.0 which means that the condition of the bearing still acceptable, however both values are increases from 2.15 to 2.225 for bearing 6203 open and 2.3477 to 2.469 for bearing 6203Z. Kurtosis increase as the severity of the defect increase [16]. It indicates that the bearing is in incipient stage of deteriorating. While for inner defect condition, the kurtosis value is 3.9977. It indicates that the bearing is in bad condition and need replacement. RMS value will increase as the condition of the defect became worst. The value of the RMS increase for unhealthy bearing compare to healthy bearing.

4.4. Results: Actual Motor Testing

4.4.1. Experiment 1

Actual motor testing was conducted using 7HP electrical motor with no load. It was operated using different speed at room temperature. The sensor was placed on the housing of the motor's bearing. The result below was acquired from oscilloscope which the motor operated at speed of 2200 rpm, 2400 rpm and 2600rpm. The graph represents voltage (V) versus time (ms).

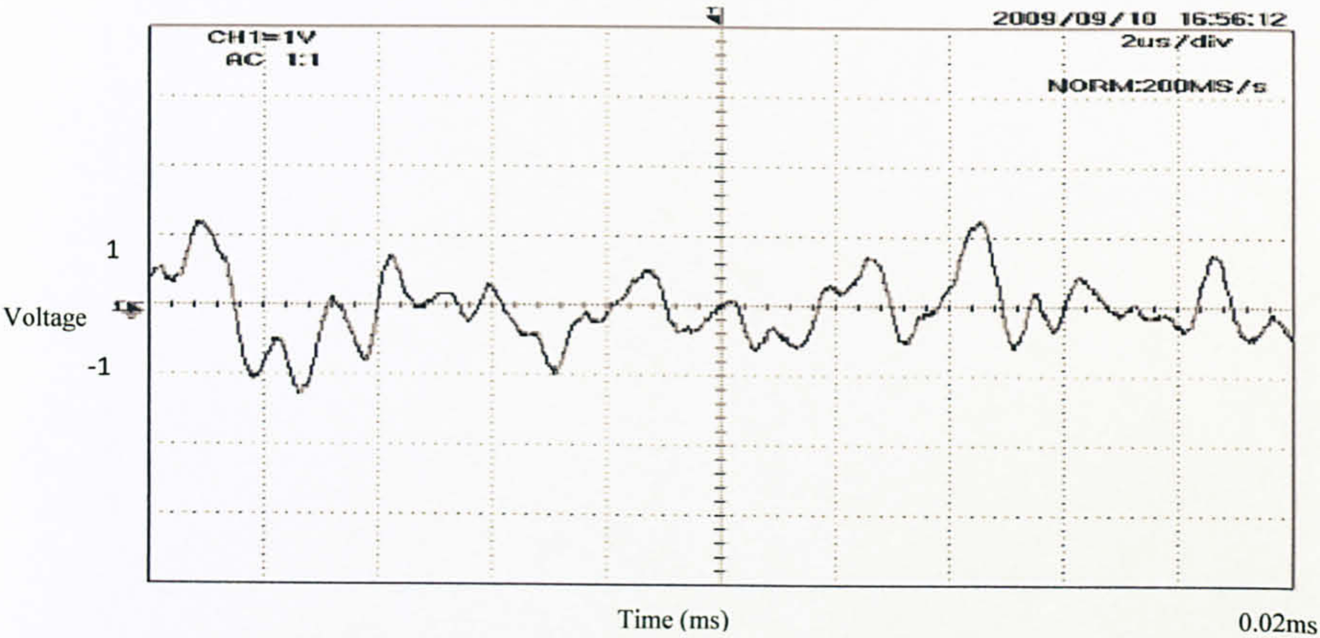

Figure 4.14: 7 HP motor bearing signal output. The motor operated at speed of 2200 rpm.

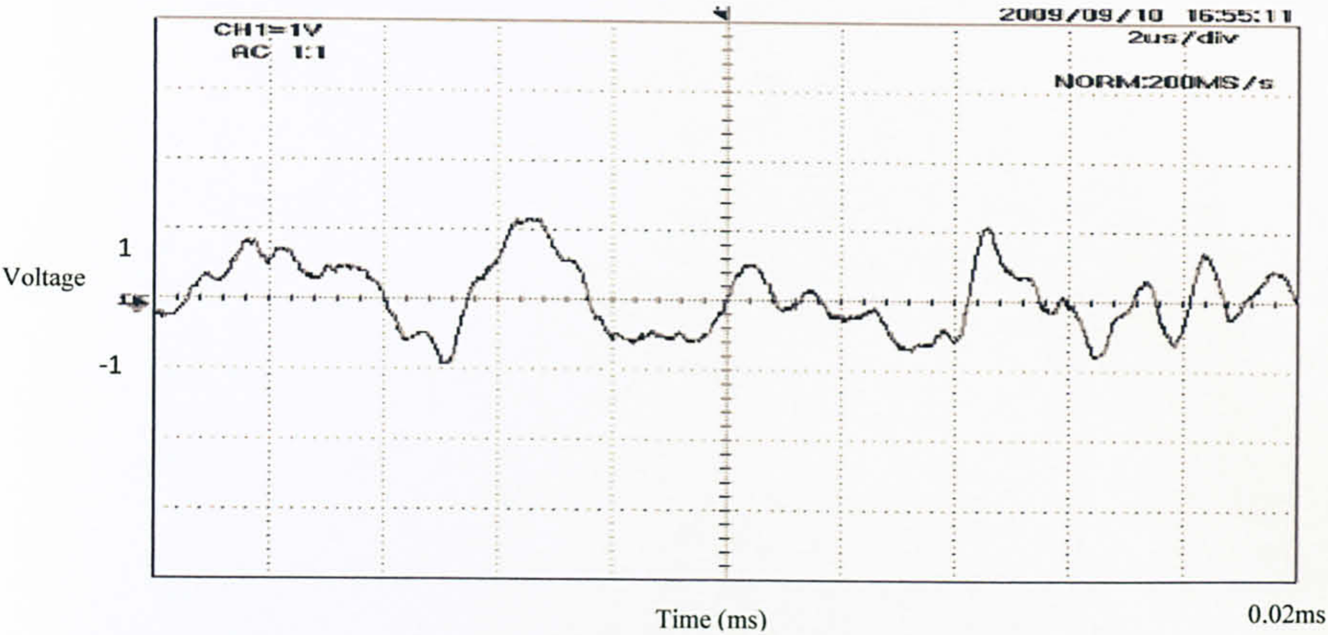

Figure 4.15: 7 HP motor bearing signal output. The motor operated at speed of 2400 rpm.

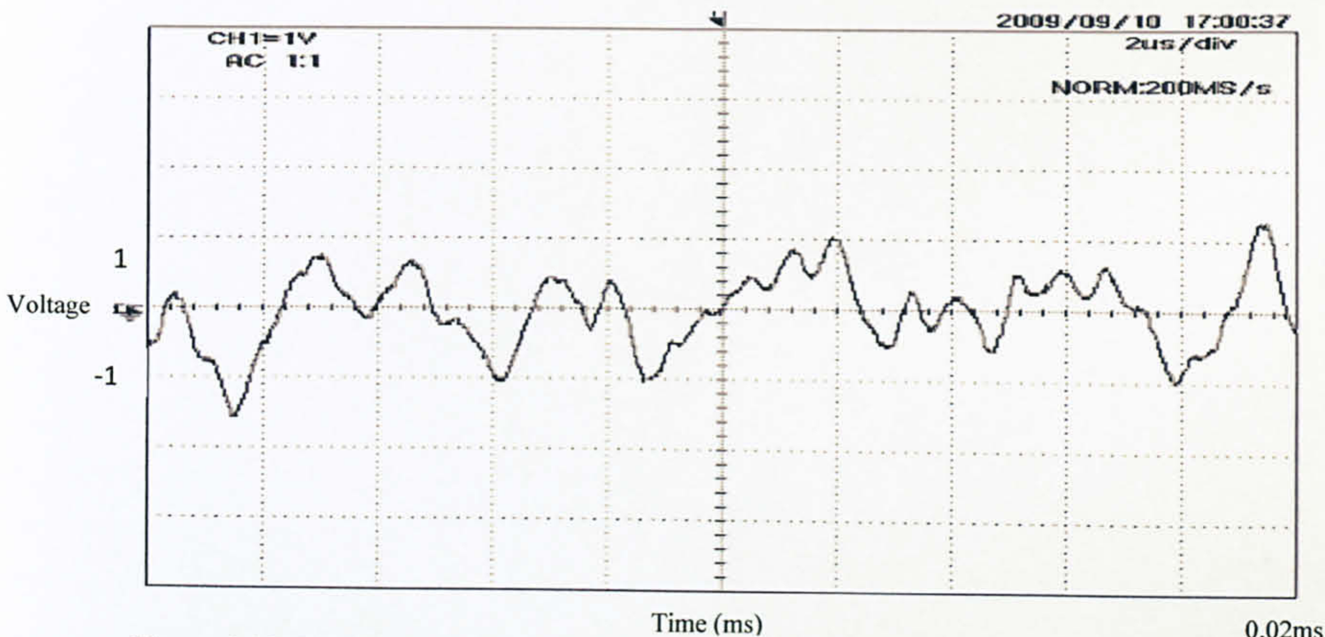

Figure 4.16: 7 HP motor bearing signal output. The motor operated at speed of 2600 rpm.

4.4.2. Experiment 2

Experiment 2 was conducted after 7HP motor was place in room temperature for one week. 7HP motor with no load was operated at different speed in room temperature. The sensor was placed on the housing of the motor's bearing. The signals were taken using data acquisition card (DAQ). The results below were obtained using MATLAB which the motor operated at speed of 2200 rpm, 2400 rpm and 2600rpm. The signals represent voltage (V) versus time (ms).

Figure 4.17: Time domain data at speed of 2200 rpm.

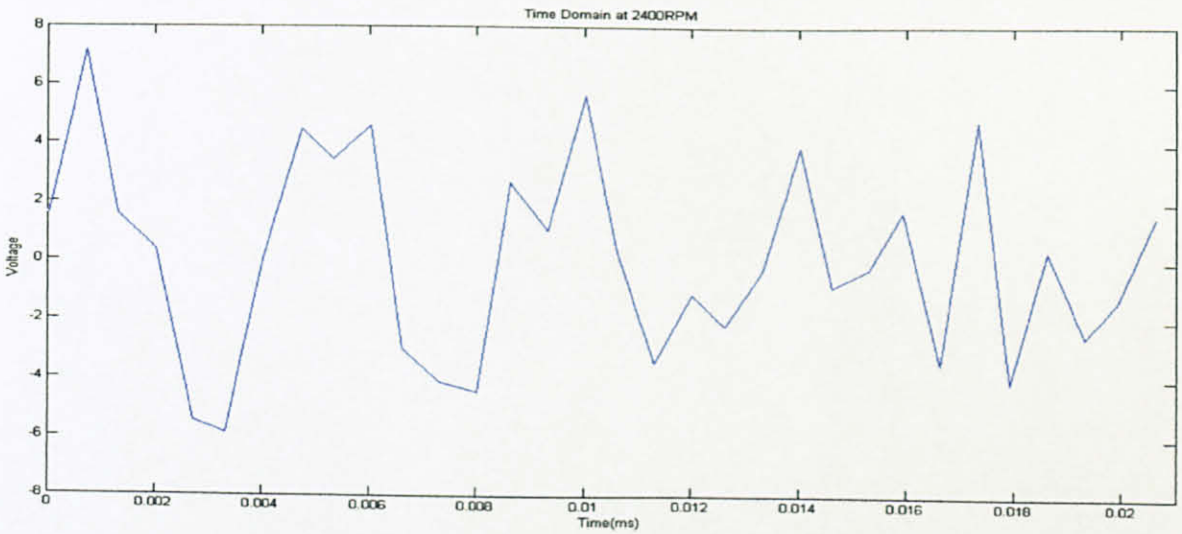

Figure 4.18: Time domain data at speed of 2400 rpm.

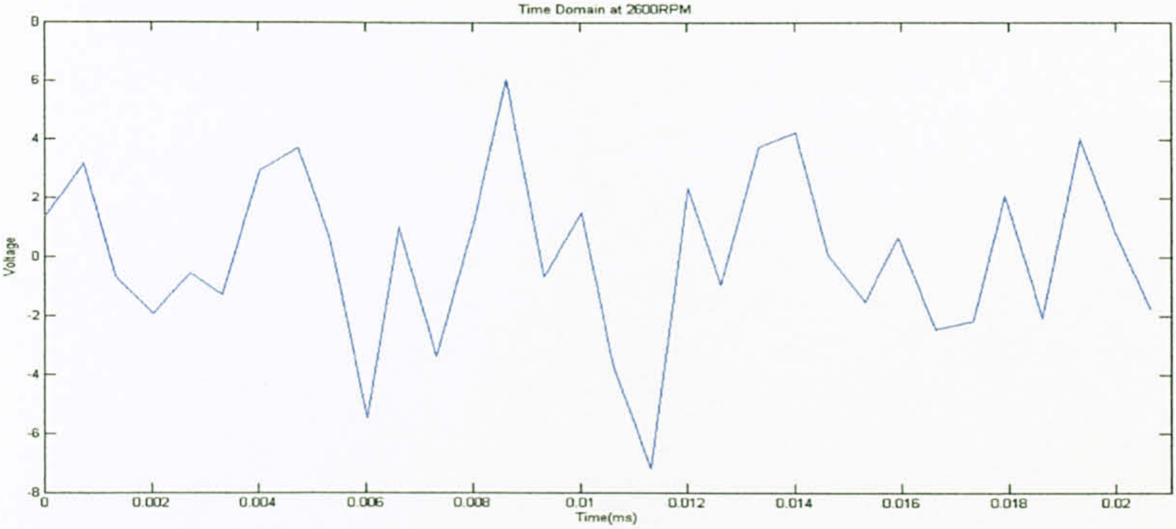

Figure 4.19: Time domain data at speed of 2600 rpm.

4.5 Discussion: Actual Motor Testing

Three analyses that need to be done, as following:

a) Time domain data
b) Statistical Analysis
c) Magnitude response

4.5.1. Time Domain Data

The table below indicates the difference in time domain data in Experiment 1 and Experiment 2.

Table 4.5: Actual motor testing (Time Domain)

Experiment 1(Before)	Experiment 2(After)
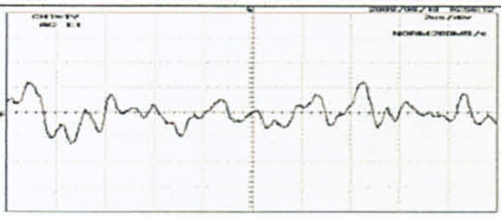	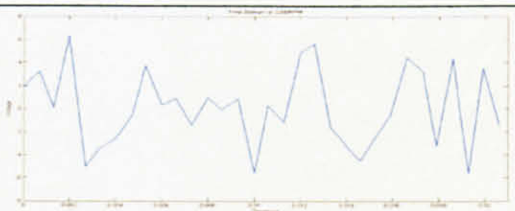
Speed: 2200rpm	
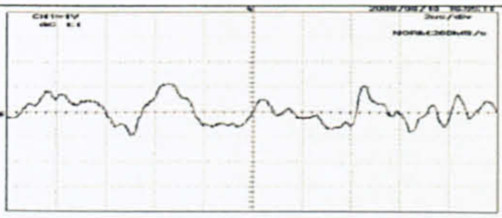	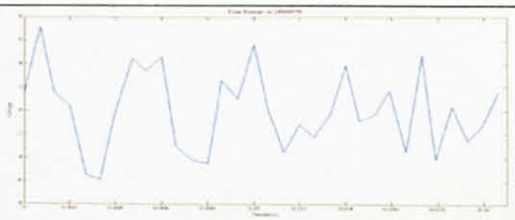
Speed: 2400rpm	
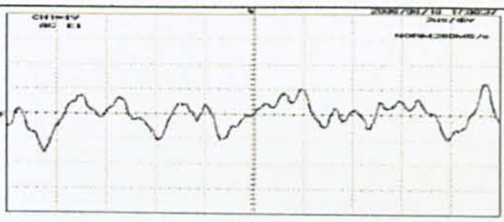	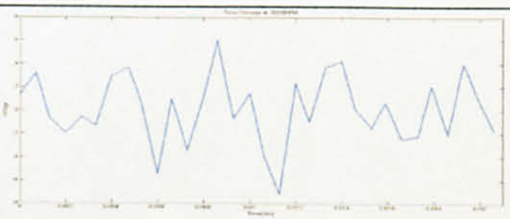
Speed: 2600rpm	

It is observed that the peak to peak voltage for Experiment 1 and Experiment 2 differ. Peak to peak voltage for Experiment 1 is less than 2.0V while peak to peak voltage for Experiment 2 is between 6.0V to 8.0V. It shows that the presence of noise is much greater in Experiment 2 compared from Experiment 1. The possible cause for this event is maybe due to the unsuitable environment for the motor.

4.5.2. Statistical Analysis

Statistical analysis is done for Experiment 2 using two statistical parameters which are kurtosis and RMS value. However, the statistical data for Experiment 1 cannot be calculated due to different type of data acquisition in Experiment 1. Thus this analysis is calculated only for Experiment 2.

Table 4.6: Actual motor testing (Statistical Analysis)

Speed	**Kurtosis**	**RMS**
2200 RPM	2.0771	0.5845
2400 RPM	2.2005	0.5923
2600 RPM	2.9005	0.5990

The table above shows the kurtosis value and RMS value for Experiment 2 in different speeds. Kurtosis values for three different speeds are less than 3.0 which indicate that the bearing of the motor is in a good condition. However, from observation, the kurtosis value at 2600RPM is near 3.0 which indicate that the possibility of incipient stage of defect in the bearing of the motor may began.

4.5.3. Magnitude Response

The magnitude response is performed only for Experiment 2 due to different set of data acquisition in Experiment 1. Below are the magnitude responses for three different speeds.

Table 4.7: Actual motor testing (Magnitude Response)

Magnitude Response
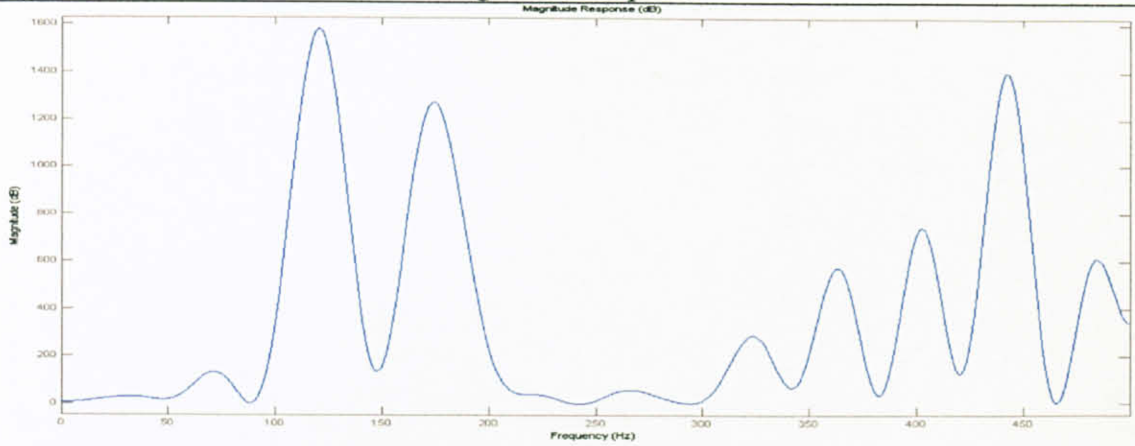
2200 RPM
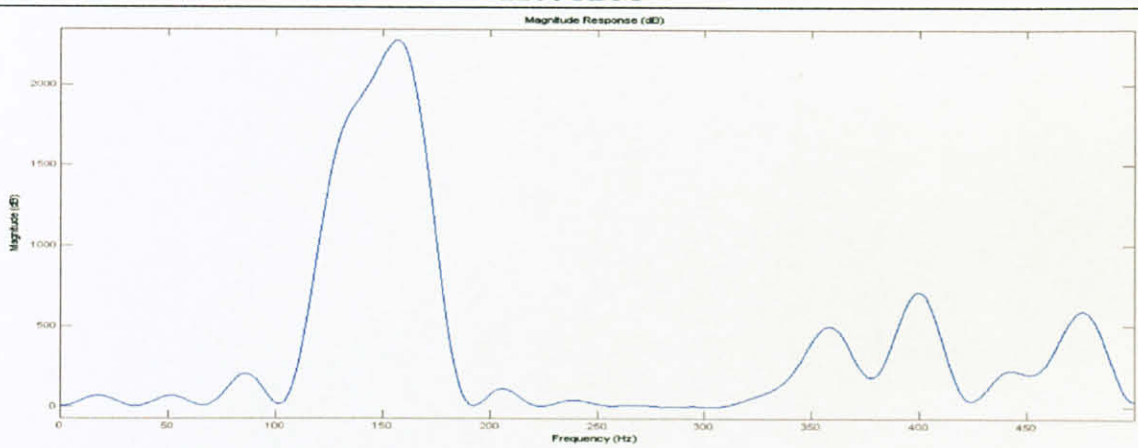
2400 RPM
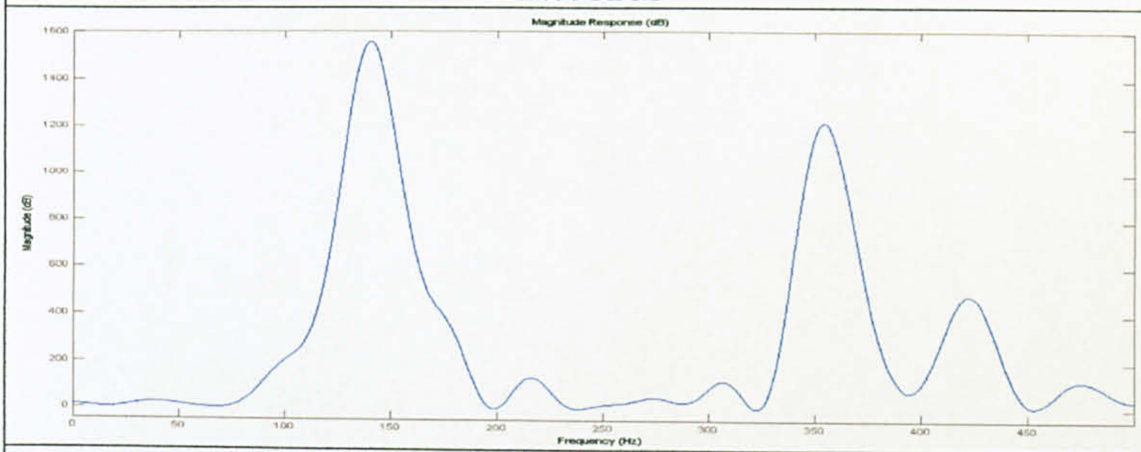
2600 RPM

These magnitude responses were developed from the signal captured from the same bearing of the motor. The magnitude responses are varying according to speeds. There are differences in patterns of the magnitude responses for the same motor. There is no significant pattern that can predict the possible condition for the motor. This shows that the magnitude response technique is not suitable for analyzing data in different speeds.

4.6 Challenges and Difficulty

There are a few problems occur during the execution of the project. The obstacles provide limited output production. The following are the obstacles faced:

a) The development of filter and amplifier using Simulink, MATLAB is unsuccessful.
   1. As a result, all the analyses are performed using raw signals.
   2. Frequency domain cannot be used to evaluate data.

b) The casing of the sensor crack.
   1. Consequently, the continuation of the experiment cannot be done due to the changes of sensitivity of the sensor.
   2. This resulted unreliable data.

CHAPTER 5

CONCLUSION AND RECOMMENDATION

5.1 Conclusion

Experiments were conducted using bench top setup to acquire the data from different types of bearing with several fault created on the bearing such as inner defect and poor lubrication. The flaw can be seen from time domain data itself where the data from a defect bearing will produce a much higher amplitude voltage as well as a few peaks in the signal. To ensure that the bearing is defect, the pattern of output signals is obtained and analyzed using magnitude response and statistical analysis. The results from magnitude response illustrate a few signatures or pattern according to the bearing condition. Statistical analysis is performed using statistical parameters which are RMS and kurtosis value. Motor breakdown and plant shutdown can be prevented if early detection of bearing is implemented. Data gathering from observation of actual motor testing have been performed as well for a 7HP motor courtesy for Maintenance Department of UTP. The results show that the amplitude response is not a suitable technique to identify data if the experiment is done at different speeds. The project has met all the objectives. Acoustic emission technique is used to detect faulty bearing. The causes of unhealthy data are predicted. There are three different signatures obtained from three different types of bearing from three conditions which are healthy, poor lubrication and inner defect bearing. As a conclusion, a set of a database has developed based on experiments done and acoustic emission technique is proved to be a suitable technique for detecting fault in bearing even at the beginning stage of deteriorating.

5.2 Recommendation

For future work, it is recommended to develop a set of amplifier and band pass/low pass filter using MATLAB to acquire the signal and analyzing it using Fast Fourier Transform (FFT). A filtered signal would eliminate unnecessary noise and significant peaks due to the fault can be detected. These significant peaks are then obtained to get the characteristic of bearing fault using FFT. Through FFT, the signature of the signal is much more apparent and clear based on the type of fault accordingly.

REFERENCES

[1] Michael J. Devaney & Levent Eren, December 2004, Detecting Motor Bearings Fault, *IEEE Instrumentation & Measurement Magazine*, vol.7, no.4, pp. 30-36.

[2] C. James Li & S.Y. Li, 1995, *Acoustic emission analysis for bearing condition monitoring*, pp. 67-74.

[3] Randy R. Schoen & Thomas G. Habetler & Farrukh Kamran & Robert G. Bartheld, 1995, Motor bearing damage using stator current, *IEEE Transactions on Industry Applications*, vol. 31, no 6, pp. 1274-1279.

[4] John S. Hsu (Htsui) & Jan Stein, 1994, Effects of eccentricities on shaft signals studied through windingless rotors, *IEEE Transactions on Energy Conversion*, Vol. 9, No. 3, pp. 564 – 571.

[5] M. Elforjani & D. Mba, 2009, Detecting natural crack initiation and growth in slow speed shafts with the Acoustic Emission technology, *Engineering Failure Analysis,* pp. 2121-2129.

[6] Austin H. Bonnett, September/October 2000, Root cause AC motor failure analysis with a focus on shaft failures, *IEEE Transactions on Industry Applications,* vol. 36, no. 5, pp. 1435-1448.

[7] Mohammed Abdalla Adam Elmaleeh & Nordin bin Saad, 2008, A study of acoustic emission technique on incipient detection of rotating machine faults, *ICARCV*, pp. 1965-1970.

[8] Michael J. Devaney & Levent Eren, December 2004, Detecting Motor Bearings Fault, *IEEE Instrumentation & Measurement Magazine*, vol.7, no.4, pp. 30-36.

[9] A. Choudhury & N. Tandon, January 2000, Application of acoustic emission technique for the detection of defects in rolling element bearings, *Tribology International*, vol. 33, pp. 39-45.

[10] C. James Li & S.Y. Li, January 2005, Acoustic emission analysis for bearing condition monitoring, *Wear*, vol.185, pp. 67-74.

[11] Mohammed Abdalla Adam Elmaleeh & Nordin bin Saad, 2008, *Acoustic emission technique for early detection of bearing faults using Labview*, [1-5].

[12] Rolf Hoppler & Reinhold A. Errath, 2007, Motor Bearings, not just a piece of metal, *2007 IEEE-IAS/PCA Cement Industry Conference*, [1-20].

[13] Austin H. Bonnet, 1992, Cause and analysis of bearing failures in motor, *U.S. Electrical Motors Division of Emerson Electric*, pp. 87-95.

[14] Palmeblads Tryckeri AB, 1994, Bearing failures and their causes, *SKF Product Information 401*, pp. 3-43.

[15] N. Tandon, G.S. Yadava & K.M. Ramakrishna, 2007, A comparison of some condition monitoring techniques for the detection of defect in induction motor ball bearings, *Mechanical Systems and Signal Processing*, vol. 21, pp. 244–256.

[16] Abdullah M. Al-Ghamd & David Mba (2006), A comparative experimental study on the use of acoustic emission and vibration analysis for bearing defect identification and estimation of defect size, *Mechanical Systems and Signal Processing*, vol. 20, pp. 1537–1571.

[17] N. Tandon & A. Choudhury, 1999, A review of vibration and acoustic measurement methods for the detection of defects in rolling element bearings, *Tribology International*, vol. 32, pp. 469–480.

[18] O V Thorsen & M Dalva, September 1997, Condition monitoring methods, failure identification and analysis for high voltage motors in petrochemical industry , *Conference Publication No.444*, pp. 109-113.

[19] Wei Zhou, Thomas G. Habetler & Ronald G. Harley, 2007, *Bearing Condition Monitoring Methods for Electric Machines: A General Review*, pp. 3-6.

[20] The shock pulse method for determining the condition of antifriction bearings, *SPM Technical Information*. Sweden: SPM Instruments AB.

[21] Jason R. Stack, Thomas G. Habetler & Ronald G. Harley, *June 2004,* Fault Classification and Fault Signature Production for Rolling Element Bearings in Electric Machines, *IEEE Transactions on Industry Applications,* Vol. 40, No. 3, pp. 735-739.

[22] Alireza Sadoughi, Soheil Tashakkor & Mohammad Ebrahimi, 2006, Intelligent Fault Diagnosing of Bearings in Rotating Machinery (a Novel Approach), *ICEM*, Vol. 422, pp. 1-6.

[23] Pratesh Jayaswal, A. K.Wadhwani & K. B.Mulchandani, 2008, Electrical Machine Analysis, *International Journal of Rotating Machinery*, Volume 2008, Article ID 583982, pp. 1-10.

[24] Xiaoli Li, 2002, A brief review: acoustic emission method for tool wear monitoring during turning, *International Journal of Machine Tools & Manufacture*, Volume 42, pp. 15-165.

[25] Takeyasu, Kazuchiro, Higuchi Yuki, 2005, Analysis of the behavior of kurtosis, *Osaka Prefecture University Education and Research Archives*, pp. 17-27.

[26] Qu,L. & He. Z, 1986, Mechanical Diagnosis, *Shanghai Science and Technology Press*, Shanghai P.R. China.

[27] Hadjileontiadis, L.J. & Douka, E., Kurtosis Analysis for Crack Detection in Thin Isotropic Rectangular Plates, *Engineering Structures*, Vol. 29, Issue 9, September 2007, pp. 2353-2364.

[28] Meng, L.L. and Si, X.J., An Improved Algorithm of Modulation Classification for Digital Communication Signals Based on Wavelet Transform, *Proceedings of the 2007 International Conference on Wavelet Analysis and Pattern Recognition, Beijing, China, 2-4 Nov. 2007*, pp.1226-1231.

[29] Bearing Failure and Causes, *Wilcoxon Research*, pp. 1- 13.

[30] Lingxin Li, C. K. Mechefske & Weidong Li, 2004, Electric motor faults diagnosis using artificial neural networks, *Insight*, Vol. 46, Issue 10, 2007, pp. 1-6.

[31] R R Schoen, T G Habetler, F Kamran a& R G Barthel, 1995,Motor bearing damage detection using stator current monitoring, *IEEE Transactions on Industrial Application*, Vol 31, No 6, pp.1274-1279.

[32] Weidong Li & Chris K. Mechefske, January 2006, Detection of induction motor stator winding and unbalance faults using hybrid method, *International of Journal of COMADEM*, Vol 9, pp.30-36.

[33] Bo Li, Mo-Yuen Chow, Yodyium Tipsuwan & James C Hung, 2000, Neural-network-based motor rolling bearing fault diagnosis, *IEEE Transactions on Industrial Electronics*, Vol 47, No 5, pp1060-1068.

[34] X. Chiementin, B. Charnley, S.Lignon & J.P. Dron, June 2010, Effect of Denoising on Acoustic Emission Signal, *Journal of Vibration and Acoustics*, Vol 132, pp. 1-9.

[35] Zulkifli Mohd Nopiah, Muhammad Ihsan Khairir, Shahrum Abdullah, Che Ku Eddy Nizwan & Mohd Noor Baharin, June 2009, Peak-Valley Segmentation Algorithm for Kurtosis Analysis and Classification of Fatigue Time Series Data, *Eurojournal Publishing Inc*, Vol 29, No. 1, pp. 113-125.

APPENDICES

APPENDIX 1: Suggested Milestone for the First Semester of 2-Semester Final Year Project

No.	Detail/ Week	1	2	3	4	5	6	7	8	9	10	11	12	13	14
1	Selection of Project Topic	■	■												
2	Preliminary Research Work		■	■	■										
3	Submission of Preliminary Report				●										
4	Research Work					■	■	■							
5	Actual Motor Testing					■	■	■							
6	Submission of Progress Report								●						
7	Actual Motor Testing									■	■				
8	Experimental Work (Data Acquisition)								■	■	■	■	■		
9	Submission of Interim Report Final Draft														
														●	
10	Oral Presentation														
															●

● Suggested milestone

■ Process

APPENDIX II: Suggested Milestone for the Second Semester of 2-Semester Final Year Project

No.	Detail/ Week	1	2	3	4	5	6	7	8	9	10	11	12	13	14
1	Experimental Setup (Different bearing)	■	■	■											
2	Experimental Setup (Different bearing)			■	■										
3	Submission of Progress Report 1				●										
4	Experimental Work (Data Acquisition)					■	■	■							
5	Data Analysis					■	■	■							
6	Submission of Progress Report								●						
7	Data Analysis								■	■	■	■	■	■	
8	Poster Exhibition												●		
9	Submission of Interim Report Final Draft													●	
10	Oral Presentation														●

● Suggested milestone

■ Process

APPENDIX III : Bench Top Setup

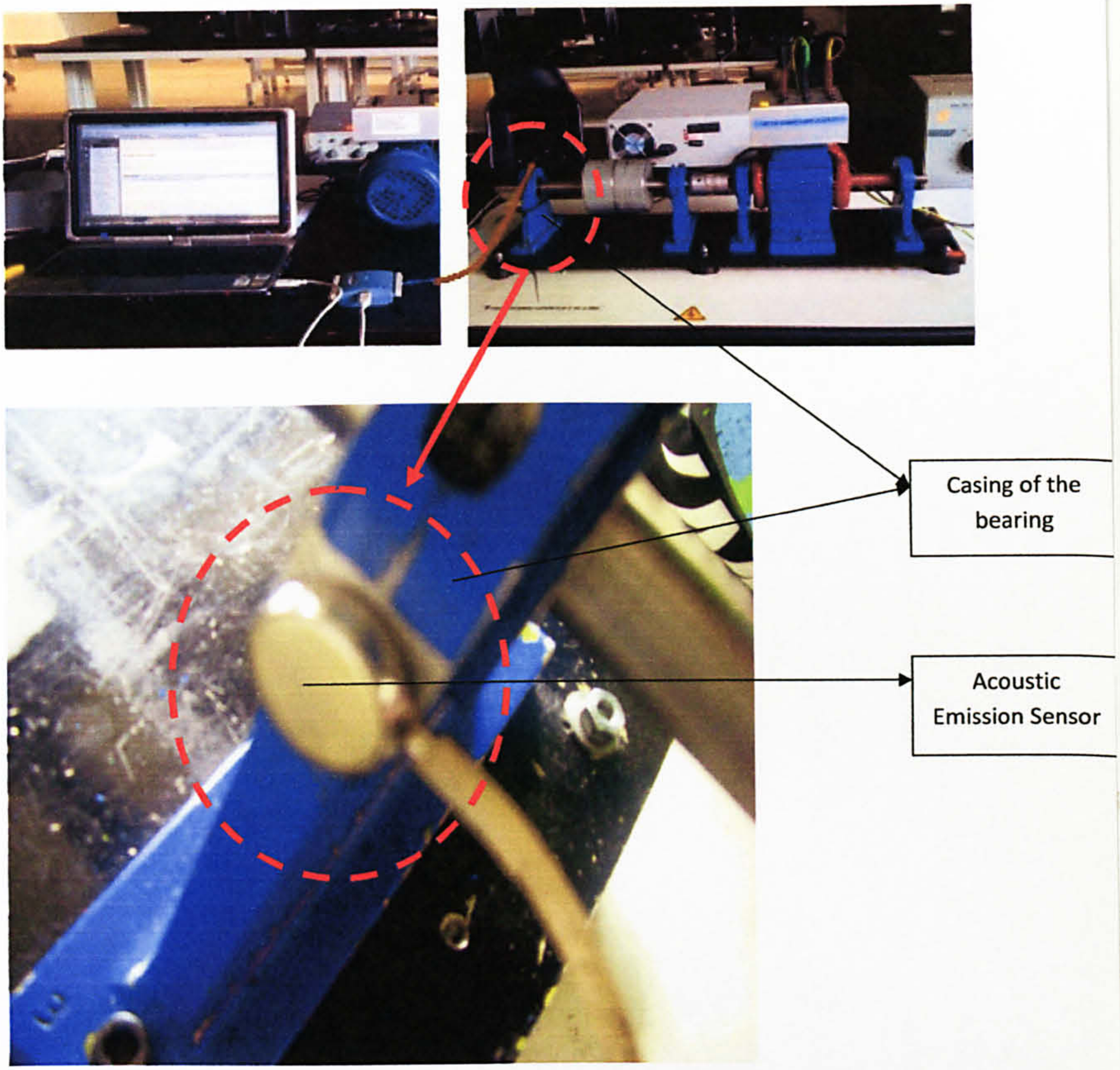

APPENDIX IV: Actual Motor Testing

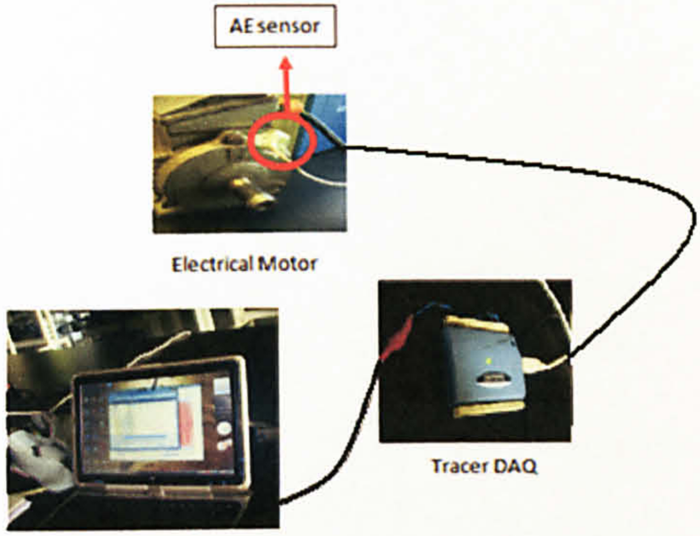

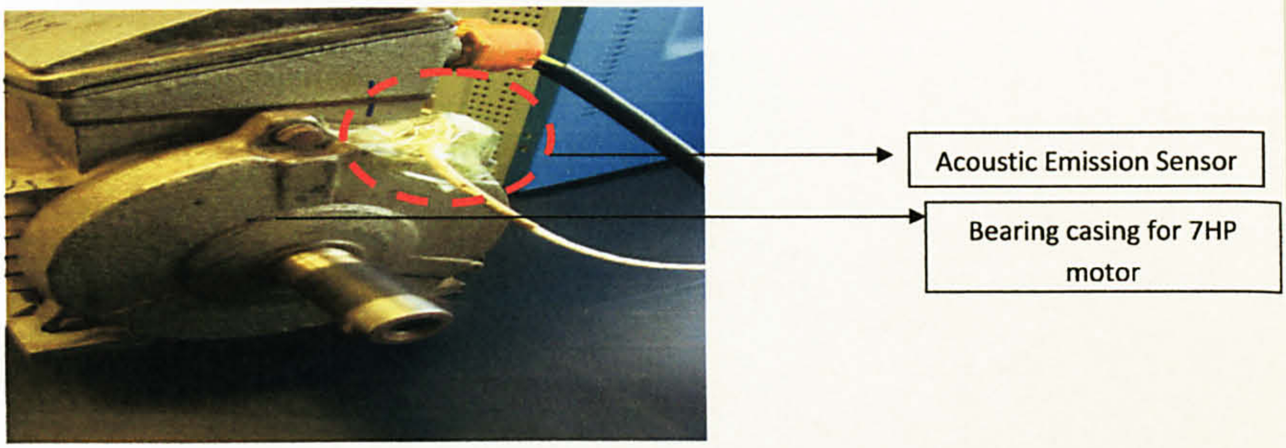

APPENDIX V: Types of bearings

Type: 6203 Open

Fault: Poor lubrication

Type: 6203 Z

Fault: Inner defect

Type: 6203 RS

Fault: Healthy

APPENDIX VI

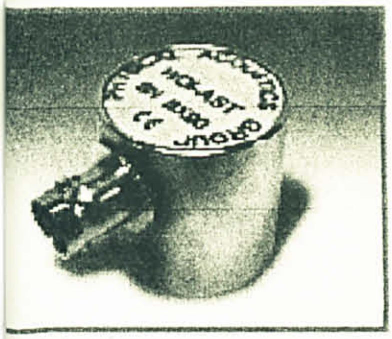

WDI Sensor

Integral Preamplifier

Acoustic Emission Sensor

escription and Features

\C's integral preamp sensors were specifically engineered) attain high sensitivity and have the capability to drive ng cables without the need for a separate preamplifier. corporating a low-noise input, 40 dB preamplifier and a ter all inside the sensor housing, these transducers are ɔmpletely enclosed in metal stainless steel (or aluminum) ɔusings that are treated to minimize RFI/EMI interference. are has also been taken to thermally isolate the critical put stage of the preamplifier in order to provide excellent ·mperature stability over the range of -35° to 75° C.

ıeir integrated Auto Sensor Test (AST*) capability allows ıese sensors to pulse as well as receive. This feature lets ɔu verify the sensor coupling and performance at any time ıroughout the test.

pplications

/ideband sensors are typically used in research applications ıd other applications where a high fidelity AE response is ·quired. In research applications, wideband AE sensors re useful where frequency analysis of the AE signal is re- uired and to help determine the predominant frequency and of AE sources for noise discrimination and selection f a suitable lower cost, general purpose AE sensor. In high delity applications, wideband sensors can detect various E wavemodes to provide more information about the AE ɔurce and distance of the AE event.

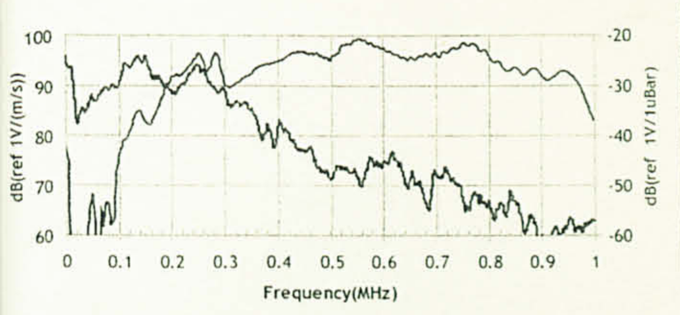

requency response of the WDI. Calibration based on ASTM E1106; alibration based on ASTM E976.

Operating Specifications

Peak Sensitivity, Ref V/(m/s) .... 96 dB
Peak Sensitivity, Ref V/μbar .... -25 dB
Operating Frequency Range .... 100 - 1000 kHz
Directionality.................................. +/-1.5 dB

Environmental

Temperature Range .... -35 to 75°C
Shock Limit .... 500 g
Completely shielded crystal for maximum RFI/EMI immunity

Physical

Dimensions.................. 1.13" diameter x 1.16" h
....(29 x 30 mm)
Weight..70 grams
Case Material..................... Stainless Steel (304)
Face Material...................................Ceramic
Connector...BNC
Connector Locations ....Side

Ordering Information and Accessories

WDI.. WDI
Cable (specify cable length) ....1234 - X
Magnetic Hold-Down MHR6I
Amplifier AE2A

Sensors include

NIST Calibration Certificate & Warranty

** AST – Auto Sensor Testing feature allows AE systems to control the sensor as a pulser and a receiver at the same time. It can therefore characterize its own condition as well as send out a simulated acoustic emission wave that other sensors can detect, so the condition of the nearby sensors also can be tested.*

PHYSICAL ACOUSTICS CORPORATION

195 Clarksville Road, Princeton Junction, NJ 08550 • Phone: 609-716-4000
Fax: 609-716-0706 • Email: sales@pacndt.com • Internet: www.pacndt.com

ISO 9001

A Member of the MISTRAS Group In

USB-1208FS

Low-cost, USB-based Module with 8 Channels, 12-bit Input

User's Guide

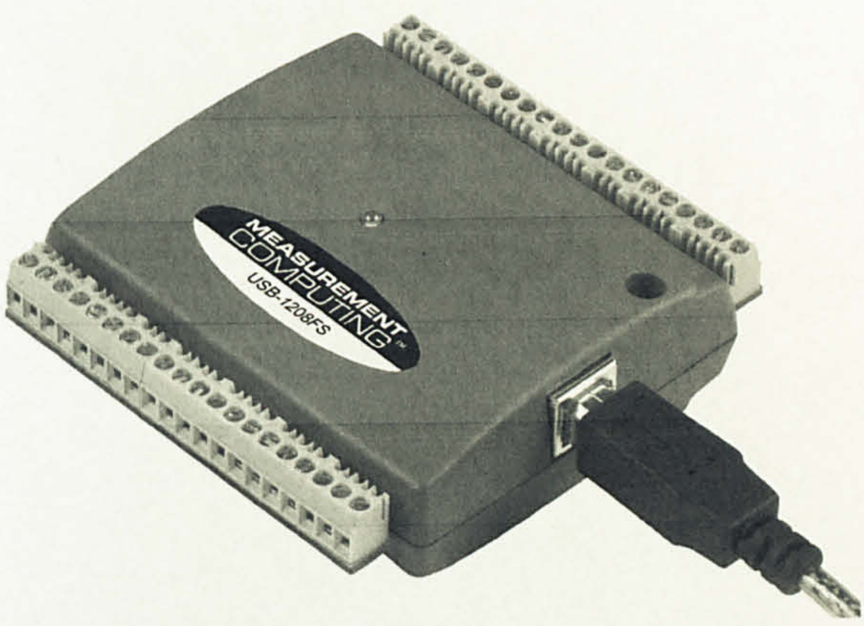

MEASUREMENT COMPUTING.

Specifications

Typical for 25°C unless otherwise specified.

Specifications in *italic text* are guaranteed by design.

Analog input

Table 1. Analog input specifications

Parameter	Conditions	Specification
A/D converter type		Successive approximation type
Input voltage range for linear operation, single-ended mode	CHx to GND	±10 volts (V) max
Input common-mode voltage range for linear operation, differential mode	CHx to GND	-10 V min, +20 V max
Absolute maximum input voltage	*CHx to GND*	*±28 V max*
Input impedance		*122KOhm*
Input current (Note 1)	Vin = +10 V	70 microamperes (μA) typ
	Vin = 0 V	-12 μA typ
	Vin = -10 V	-94 μA typ
Number of channels		8 single-ended / 4 differential, software selectable
Input ranges, single-ended mode		±10 V, G=2
Input ranges, differential mode		±20 V, G=1 ±10 V, G=2 ±5 V, G=4 ±4 V, G=5 ±2.5 V, G=8 ±2.0 V, G=10 ±1.25 V, G=16 ±1.0 V, G=20 Software selectable
Throughput (Note 2)	Software paced	250 samples per second (S/s) typ, PC-dependent
	Continuous scan	50 kilosamples per second (kS/s)
Channel gain queue	Up to 16 elements	Software configurable channel, range, and gain.
Resolution (Note 3)	Differential	12 bits, no missing codes
	Single-ended	11 bits
CAL accuracy	CAL = 2.5 V	±36.25 mV max
Integral linearity error		±1 least significant bit (LSB) typ
Differential linearity error		±0.5 LSB typ
Repeatability		±1 LSB typ
CAL current	Source	5 milliamperes (mA) max
	Sink	20 μA min, 100 μA typ
Trigger source	Software selectable	External digital: TRIG_IN
Pacer source	Software selectable	Internal External (SYNC), rising edge triggered Programmed IO

Note 1: Input current is a function of applied voltage on the analog input channels. For a given input voltage, V_{in}, the input leakage is approximately equal to $(8.181*V_{in}-12)$ μA.

Note 2: Maximum throughput scanning to PC memory is machine dependent. The rates specified are for Windows XP only. Maximum rates on operating systems that predate XP may be less and must be determined through testing on your machine

Note 3: The AD7870 converter only returns 11-bits (0-2047 codes) in single-ended mode.

Table 2. Accuracy, differential mode

Range	Accuracy (LSB)
±20 V	5.1
±10 V	6.1
±5 V	8.1
±4 V	9.1
±2.5 V	12.1
±2 V	14.1
±1.25 V	20.1
±1 V	24.1

Table 3. Accuracy, single-ended mode

Range	Accuracy (LSB)
±10 V	4.0

Table 4. Accuracy components, differential mode - All values are (±)

Range	% of Reading	Gain Error at full scale (FS) (millivolts (mV))	Offset (mV)	Accuracy at FS (mV)
±20 V	0.2	40	9.766	49.766
±10 V	0.2	20	9.766	29.766
±5 V	0.2	10	9.766	19.766
±4 V	0.2	8	9.766	17.766
±2.5 V	0.2	5	9.766	14.766
±2 V	0.2	4	9.766	13.766
±1.25 V	0.2	2.5	9.766	12.266
±1 V	0.2	2	9.766	11.766

Table 5. Accuracy components, single-ended mode - All values are (±)

Range	% of Reading	Gain Error at FS (mV)	Offset (mV)	Accuracy at FS (mV)
±10 V	0.2	20	19.531	39.531

Table 6. Noise performance, differential mode

Range	Typical counts	Least significant bit$_{\text{root mean square}}$ (LSB_{rms})
±20 V	2	0.30
±10 V	2	0.30
±5 V	3	0.45
±4 V	3	0.45
±2.5 V	4	0.61
±2 V	5	0.76
±1.25 V	7	1.06
±1 V	8	1.21

Table 7. Noise performance, single-ended mode

Range	Typical Counts	LSB_{rms}
±10 V	2	0.30

Analog output

Table 8. Analog output specifications

Parameter	Conditions	Specification
Resolution		12-bits, 1 in 4096
Output range		*0 – 4.096 V, 1 mV per LSB.*
Number of channels		2
Throughput (Note 4)	Software paced	250 S/s single channel typical, PC dependent
	Single channel, continuous scan	10 kS/s
	Dual channel, continuous scan, simultaneous update	5 kS/s
Power on and reset voltage		Initializes to 000h code
Output drive	Each D/A OUT	15 mA
Slew rate		0.8V/microsecond (μs) typ

Note 4: Maximum throughput scanning to PC memory is machine dependent. The rates specified are for Windows XP only. Maximum rates on operating systems that predate XP may be less and must be determined through testing on your machine.

Table 9. Analog output accuracy, all values are (±)

Range	Accuracy (LSB)
0-4.096 V	4.0 typ, 45.0 max

Table 10. Analog output accuracy components, all values are (±)

Range	% of FSR	Gain Error at FS (mV)	Offset (mV) (Note 5)	Accuracy at FS (mV)
0-4.096 V	0.1 typ, 0.9 max	4.0 typ, 36.0 max	1.0 typ, 9.0 max	4.0 typ, 45.0 max

Note 5: Negative offsets will result in a fixed zero-scale error or "dead band." At the maximum offset of -9 mV, any input code of less than 0x009 will not produce a response in the output.

Digital input/output

Table 11. Digital I/O specifications

Digital type	CMOS
Number of I/O	16 (Port A0 through A7, Port B0 through B7)
Configuration	2 banks of 8
Pull up/pull-down configuration	All pins pulled up to Vs via 47K resistors (default). Positions available for pull down to ground. Hardware selectable via zero ohm (Ω) resistors as a factory option.
Input high voltage	2.0 V min, 5.5 V absolute max
Input low voltage	0.8 V max, –0.5 V absolute min
Output high voltage (IOH = -2.5 mA)	3.8 V min
Output low voltage (IOL = 2.5 mA)	0.7 V max
Power on and reset state	Input

External trigger

Table 12. Digital trigger specifications

Parameter	Conditions	Specification
Trigger source (Note 6)	External Digital	TRIG_IN
Trigger mode	Software selectable	Edge sensitive: user configurable for CMOS compatible rising or falling edge.
Trigger latency		10 µs max
Trigger pulse width		1 µs min
Input high voltage		4.0 V min, 5.5 V absolute max
Input low voltage		1.0 V max, –0.5 V absolute min
Input leakage current		*±1.0 µA*

Note 6: TRIG_IN is a Schmitt trigger input protected with a 1.5 kilohm (kΩ) series resistor.

External clock input/output

Table 13. External clock I/O specifications

Parameter	Conditions	Specification
Pin name		SYNC
Pin type		Bidirectional
Software selectable direction	Output (default)	Outputs internal A/D pacer clock.
	Input	Receives A/D pacer clock from external source.
Input clock rate		50 KHz, maximum
Clock pulse width	Input mode	1 µs min
	Output mode	5 µs min
Input leakage current	*Input mode*	*±1.0 µA*
Input high voltage		4.0 V min, 5.5 V absolute max
Input low voltage		1.0 V max, –0.5 V absolute min
Output high voltage (Note 7)	IOH = -2.5 mA	3.3 V min
	No load	3.8 V min
Output low voltage (Note 7)	IOL = 2.5 mA	1.1 V max
	No load	0.6 V max

Note 7: SYNC is a Schmitt trigger input and is over-current protected with a 200 Ω series resistor.